A quantitative assessment of uncertainties affecting estimates of global mean OH derived from methyl chloroform observations

A quantitative assessment of uncertainties affecting estimates of global mean OH derived from methyl chloroform observations

James S. Wang,[1] Michael B. McElroy,[2] Jennifer A. Logan,[2] Paul I. Palmer,[3] William L. Chameides,[4] Yuxuan Wang,[2] and Inna A. Megretskaia[2]

Received 2 February 2007; revised 24 October 2007; accepted 6 March 2008; published 18 June 2008.

[1] We estimated the global abundance of OH for the years 1988–1994 by interpreting observations of methyl chloroform (MCF) from two networks using an inverse technique and a 3-D chemical transport model driven by assimilated meteorology. Our inversion approach optimized both the emissions of MCF and the abundance of OH. Because of an a priori overestimate of the latitudinal gradient of MCF concentration by the model in the standard setup, the inversion lowers global emissions and the global sink due to OH. Optimized emissions are about 10% lower than published inventories on average between 1988 and 1994, and the decrease in the sink suggested by the inversion implies an average lifetime for MCF (with respect to tropospheric OH) of about 6.9 years, 11–21% longer than the 5.7–6.2 years reported in previous optimization studies. Our results are driven by the need to match the observed latitudinal gradient of MCF while balancing the MCF budget. We find that these results depend on the a priori constraint placed on MCF emissions, the rate of interhemispheric mixing in the model, the interhemispheric distribution of OH assumed, and the model simulation of pollution events. Since these factors are highly uncertain, we believe that the level of understanding on global lifetimes of pollutants removed by OH is lower than might be implied by the narrow range of estimates for MCF lifetime in the literature.

Citation: Wang, J. S., M. B. McElroy, J. A. Logan, P. I. Palmer, W. L. Chameides, Y. Wang, and I. A. Megretskaia (2008), A quantitative assessment of uncertainties affecting estimates of global mean OH derived from methyl chloroform observations, *J. Geophys. Res.*, *113*, D12302, doi:10.1029/2007JD008496.

1. Introduction

[2] The hydroxyl radical (OH) is the primary "cleanser" of the atmosphere, oxidizing a number of greenhouse gases including methane (CH_4), HCFCs, and HFCs, and many other pollutants. To estimate the global abundance of OH, researchers have carried out photochemical model simulations as well as inverse approaches relying on concentration measurements of trace gases and knowledge of the kinetics of the removal of these gases by OH. In particular, measurements of CH_3CCl_3 (methyl chloroform, abbreviated MCF in this paper), an industrial solvent, have been widely used, and the resulting estimates for global OH are widely cited [*Prinn et al.*, 2001, 2005; *Spivakovsky et al.*, 2000; *Krol and Lelieveld*, 2003; *Bousquet et al.*, 2005]. The corresponding estimates for lifetime of MCF with respect to tropospheric OH are clustered around 5.7–6.2 years (see Table 1), a range of ±4%, potentially leading to the false impression that global lifetimes of pollutants are well understood. However, we suggest in this paper that these estimates are critically dependent on various assumptions and uncertain model parameters, including the reliability of estimates for MCF emissions, interhemispheric mixing rates in models, the spatial distribution of OH, and the treatment of pollution events.

[3] The motivation for the present study was provided by our previous inverse analysis of CH_4 [*Wang et al.*, 2004], which suggested that earlier studies may have overestimated the OH sink for this gas. We report here results from a similar analysis of MCF. Both analyses used an inversion approach in which the emissions of the tracer and the abundance of OH are optimized simultaneously. Most previous inversion studies in the case of CH_4 severely restricted the range over which OH could vary, or in the case of MCF did not optimize emissions. *Bousquet et al.* [2005] is an exception, allowing MCF emissions to be adjusted, but their analysis focused on the trends and interannual variations of OH rather than on the absolute level. MCF has advantages over CH_4 as a tracer for estimating OH, including the relatively well known spatial distribution of its emissions (dominated by industrial sources) and the spatial separation between the emissions and removal by OH, which minimizes correlation between the two inversion parameters and allows for a tighter

[1]Environmental Defense Fund, New York, New York, USA.
[2]Department of Earth and Planetary Sciences and School of Engineering and Applied Sciences, Harvard University, Cambridge, Massachusetts, USA.
[3]School of GeoSciences, University of Edinburgh, Edinburgh, UK.
[4]Nicholas School of the Environment and Earth Sciences, Duke University, Durham, North Carolina, USA.

0148-0227/08/2007JD008496

Table 1. Summary of Results

Study	Global Mean OH (10^5 molecules cm^{-3})[a]	MCF Lifetime With Respect to Tropospheric OH (Years)[b]	CH_4 Lifetime With Respect to All Sinks (Years)[c]
Previous optimization studies			
Spivakovsky et al. [2000]	11.6	5.7	–
Intergovernmental Panel on Climate Change (*IPCC*) [2001]	–	–	8.4
Krol and Lelieveld [2003][d]	10.3[e]	6.2[f]	–
Prinn et al. [2005][g]	11.0	5.9[h]	9.2[i]
Bousquet et al. [2005][j]	9.9	–	–
IPCC [2007]	–	–	8.7
GEOS-Chem photochemical simulations			
Martin et al. [2003]: GEOS-Chem v.4.26 1996–1997 (GEOS-Strat)	12.1	5.6	–
I. Bey (personal communication, 2004): GEOS-Chem v.5.02 1996–97 (GEOS-Strat)	11.0	6.2	–
Wu et al. [2007]: GEOS-Chem v.7.02.04 2001 (GEOS-3)	10.3	6.7	11.1
Wu et al. [2007]: (GEOS-4)	11.2	5.9	9.8
This study[k]	10.6	6.9	10.1

[a]Weighted by mass of air, unless otherwise specified.
[b]MCF lifetime with respect to tropospheric OH (total atmospheric burden/tropospheric loss).
[c]We assume a CH_4 lifetime with respect to loss in the stratosphere of 161 years and a lifetime with respect to loss in soils of 142 years [*Wang et al.*, 2004].
[d]We extract the subset of their results between 1989 and 1994 for more precise comparison with our results.
[e]Weighted by the CH_3CCl_3 + OH reaction rate.
[f]We derived the optimized lifetime using the scaling factors in Table 1 of *Krol and Lelieveld* [2003], the unoptimized tropospheric lifetimes in Table A1 of *Krol and Lelieveld* [2003], and an approximate factor of 1.1 to convert from tropospheric to atmospheric MCF burden.
[g]We extract the subset of their results between 1988 and 1994.
[h]We estimate this lifetime on the basis of the reported average of 6.0 years for the period 1979–2003, assuming lifetime is inversely proportional to OH concentration.
[i]We estimate this lifetime on the basis of the reported averages of 10.2 and 110 years with respect to loss in the troposphere and stratosphere, respectively, for the period 1979–2003, assuming lifetime is inversely proportional to OH concentration.
[j]From their "mean inversion"; we extract the results for 1988–1994.
[k]Average over 1988–1994, including GAGE and ESRL results.

constraint on their values. MCF emissions are concentrated in the northern extratropics, while OH is highest in the tropics.

[4] In the remainder of this paper we discuss details of our methods and results, examine why our results differ from previous estimates and, more broadly, assess the critical factors influencing the determination of MCF emissions and lifetime. We speculate on implications of our results for MCF emissions and pollutant lifetimes, as well as implications for the global warming potentials (GWPs) of greenhouse gases removed by OH. We do not assess long-term temporal trends in OH, an issue that has received much attention; various bottom-up and top-down analyses have produced estimates for decadal-scale trends in OH that differ widely in magnitude and even in sign [e.g., *Karlsdóttir and Isaksen*, 2000; *Prinn et al.*, 2001, 2005; *Dentener et al.*, 2003; *Krol and Lelieveld*, 2003; *Wang et al.*, 2004; *Millet and Goldstein*, 2004; *Bousquet et al.*, 2005]. We defer any discussion of the implications of our results for recent trends in OH to future papers.

2. Methods

[5] We used a Bayesian inverse approach to estimate the strength of the OH sink and the MCF source for 1988–1994. These years correspond to the meteorological fields that were available at the time of this study for one particular version of the data assimilation system (GEOS-1); this period is also interesting with regards to the evolution of atmospheric MCF, since emissions begin to decrease mid-way through the period, as discussed in detail below. We refer the reader to *Wang et al.* [2004] for a general discussion of the inverse method and of the chemical transport model (CTM). For the present study, parameters optimized include the global, annual strength of the OH sink and the magnitude of annual MCF emissions from 5 regions: North America, Europe (including the former Soviet Union), Asia (east Asia, the Middle East, and Africa north of 30°N), Northern Hemisphere tropics (all areas between 0° and 25°N in the Americas and between 0° and 30°N elsewhere), and Southern Hemisphere.

[6] The spatial and seasonal distributions of OH were taken from *Wang et al.* [2004], which in turn used a parameterization for calculating OH developed by *Duncan et al.* [2000]; these were scaled uniformly for the a priori calculation to correspond to the value for global mean OH estimated by *Spivakovsky et al.* [2000] (see Table 1 for global mean OH and trace gas lifetimes estimated by various studies). We assumed an a priori uncertainty of 15% (1σ) for the global OH sink. That particular value corresponds to an estimate for the uncertainty of global mean OH based on the MCF budget, accounting for uncertainties in the source, absolute calibration, etc. [*Spivakovsky et al.*, 2000], but it is of comparable magnitude to the uncertainty in the bottom-up, photochemical estimate for OH from the same study (e.g., the authors stated that the error in OH deriving from errors in O_3 and H_2O is not expected to exceed ±25%). We focus on the global sink rather than considering the sinks in the Northern Hemisphere (NH) and Southern Hemisphere (SH) separately since the averaging

kernels indicated that the NH sink is correlated with the sources in the north. The averaging kernels, or model resolution functions, indicate how well each parameter in an inversion can be constrained by the available information; we discuss this in more detail in section 3.2. Scaling OH by a globally uniform factor carries with it a greater risk of aggregation error. To evaluate the significance of this error, we carried out a sensitivity test using an alternative OH field (discussed below).

[7] The a priori estimates for the sources were taken from *McCulloch and Midgley* [2001]. We assumed an a priori uncertainty for the sources of 7.5% (1σ), significantly larger than that reported by *McCulloch and Midgley* [2001] ($\sim$2.5% for the late 1980s and early 1990s), since recent studies suggest significant uncertainties in our understanding of MCF emissions [*Millet and Goldstein*, 2004; *Barnes et al.*, 2003; *Krol et al.*, 2003; *Li et al.*, 2005; *Yokouchi et al.*, 2005]. While our choice of 7.5% is arbitrary, sensitivity tests suggest that it is large enough to allow for significant changes to the emissions (see section 3.4.1). The emissions were distributed spatially according to the country totals from *Midgley and McCulloch* [1995]; within countries, the emissions were distributed on the basis of population. For the grid box containing the Cape Meares, Oregon, site, we shifted the emissions one box to the east, since the presence of a major urban area in the box causes concentrations to be unrepresentative of the clean, coastal site. We had tested also sampling the grid box offshore of Cape Meares (to the west) rather than shifting emissions, and found that the inversion parameters changed in the same direction relative to the a priori values, with a smaller magnitude of change (7% and 24% smaller for the sink and global source, respectively).

[8] The distribution of MCF loss in the stratosphere due to OH and photolysis was based on results from a stratospheric model [*Schneider et al.*, 2000; D. Jones, personal communication, 2000]. The strength of the stratospheric sink was kept at a fixed value, corresponding to a lifetime averaging about 45 years [*World Meteorological Organization*, 2003]. The ocean sink for MCF was modeled as a first-order loss over ice-free ocean areas (simply assumed to include areas equatorward of 68°S and 76°N and accounting for the fraction of each surface grid box underlain by ocean), with a fixed lifetime of 85 years [*Butler et al.*, 1991]. These values are similar to those assumed in previous optimization studies, e.g., 43 years and 80 years in the study by *Spivakovsky et al.* [2000], 45 years and $\sim$90 years in the study by *Krol and Lelieveld* [2003], and 38 years and 94 years in the study by *Prinn et al.* [2005]. Thus, any major difference between the inferred loss of MCF in our study and that of the previous studies would be attributed to tropospheric OH (and a possible soil sink, discussed below). Note that the stratospheric and ocean sinks are small relative to the tropospheric OH sink. We neglected the possibility that the ocean might provide a source for MCF at high latitudes during the period of rapidly declining atmospheric concentrations [*Wennberg et al.*, 2004], since this is expected to have had greatest relative impact in the late 1990s and early 2000s, outside of the period of our analysis.

[9] Assimilated winds and other meteorological variables specific to the years of the analysis were used in the 3-D GEOS-Chem CTM [*Bey et al.*, 2001]. The work shown here employed version 5.02 of GEOS-Chem for transport, with GEOS-1 meteorological fields (http://www.as.harvard.edu/chemistry/trop/geos/geos_versions.html). The model was run at a higher resolution, 4° latitude by 5° longitude, than in previous inverse analyses of MCF (except for *Bousquet et al.* [2005]). We found through simulations of ^{85}Kr [*Wang et al.*, 2004] and SF_6 (results for the SF_6 simulation are included in Appendix A) that the model reproduces the observed latitudinal gradients of the tracers in general and thus appears to simulate interhemispheric mixing accurately. In addition, the interhemispheric exchange time for ^{85}Kr, as defined by *Prather et al.* [1987], in our model is 1.0 year, which is close to the value of 1.1 years determined by *Jacob et al.* [1987] on the basis of a CTM simulation that matched observations of ^{85}Kr. Model vertical profiles of CH_4 exhibited good agreement with observations [*Wang et al.*, 2004], suggesting that the model simulates vertical mixing reasonably well.

[10] A tagged MCF tracer run was carried out for each year using the CTM to determine the contributions of individual sources and sinks to the total MCF concentration at each site (elements of the Jacobian matrix). In the tagged runs, each source/sink was simulated separately, starting from zero concentration, emitting or destroying an amount of MCF specified by the a priori estimate over the year, and accumulating parts per trillion of MCF (negative concentrations in the case of sinks). Since the magnitudes of the OH and ocean sinks depend on total MCF concentration, we linearized the problem by specifying a 3-D, monthly varying distribution of MCF, based on observations, for the OH and ocean tracers. Specifically, the MCF distribution was derived using the following iterative procedure. A preliminary MCF distribution was taken from a posteriori concentrations for the preceding year. We performed an inversion using the output of the preliminary tagged run, and then used the a posteriori MCF concentrations in a refined tagged run for a second iteration of the inversion. For the first year of the analysis, 1988, the preliminary MCF distribution was taken from a forward model run from 1985 to 1988 using a priori sources and sinks, and initialized with a zonally uniform distribution of MCF based on observations.

[11] In addition, an ''initial condition tracer'' was run for each year to account for the effects of emissions and losses from all years prior to the year of interest. We first adopted a MCF initial condition field, constrained to match observations optimally at the beginning of the year through the inversion for the preceding year. Then this field was advected and mixed over the subsequent year with no emissions or losses. We verified that the MCF distribution summed up from the source, sink, and initial condition tracers is equivalent to that produced by a single model run in which all the sources and sinks are introduced interactively.

[12] Monthly means of high-frequency, in situ MCF observations from the GAGE and NOAA Earth System Research Laboratory (ESRL) Global Monitoring Division (GMD) (formerly CMDL) networks were used in the inverse calculations [*Prinn et al.*, 2001; *Montzka et al.*, 1996]. (Note that we did not use the independent set of ESRL flask data described by *Montzka et al.* [2000].) We used GAGE data for the years 1985–1994 and ESRL data

for 1991–1994. (We downloaded the GAGE data from http://cdiac.ornl.gov/ftp/ale_gage_Agage/GAGE/ in June 2003, and the ESRL data from ftp://ftp.cmdl.noaa.gov/hats/solvents/CH3CCl3/insituGCs/RITS/ in August 2003.) Except for one sensitivity test, we conducted separate analyses with the two data sets, since they are based on different calibration standards. The use of the two temporally overlapping data sets with their differing geographic distributions provides one kind of confirmation of the inversion results. We carried out separate initial condition and sink tracer runs for the two data sets because of the differing calibration standards. For the first year of ESRL data, 1991, the inversion relied on the initial conditions generated from the 1990 GAGE inversion; on account of the inaccuracy of the initial conditions due to the differing calibration standards, we used those inversion results only to provide initial conditions for the 1992 ESRL inversion and exclude them from the discussion below.

[13] We used monthly means that were computed using all data, including those indicative of pollution episodes. (For GAGE, we used the "polluted" monthly mean data provided.) This contrasts with the methodology of *Prinn et al.* [2001, 2005], *Krol and Lelieveld* [2003], and *Bousquet et al.* [2005], in which only nonpolluted observations were used while no analogous selection procedure was applied to model output, except for one sensitivity test in the last study in which polluted data for the Mace Head site were included. The relatively high spatial and temporal resolution of our model and the assimilated meteorology allow for fairly accurate simulation of pollution episodes and obviate the need to remove those data. Furthermore, we believe that inclusion of pollution episodes allows for a better constraint on regional MCF emissions, which in turn allows for a better constraint on the OH sink; various studies have utilized pollution events to estimate regional emissions of MCF and other halocarbons, CH_4 and other greenhouse gases, and carbon monoxide [e.g., *Simmonds et al.*, 1996; *Barnes et al.*, 2003; *Reimann et al.*, 2005]. We examined the sensitivity of the inversion results to errors in the model simulation of pollution events, as described in section 3.4.4.

[14] In calculating the monthly means, we did not sample the model according to the days for which observations are available. (For the monthly 10th percentiles used in a sensitivity test discussed in section 3.4.4, we did sample the model appropriately.) But we did exclude from the analysis the months without any observations. We conducted calculations to roughly assess the magnitude of the error deriving from the lack of sampling. For year 1988, we found that the average difference between the sampled and unsampled monthly means (the bias) ranged from −0.37 to 0.07 ppt across the sites, or −0.28 to 0.06% of the mean concentrations, and that the standard deviation of the differences between the sampled and unsampled means ranged from 0.36 to 1.19 ppt, or 0.34 to 0.93%. On the basis of these numbers, we believe that missampling does not significantly affect the inversion results.

[15] We used an original formulation to estimate the observation error as the sum of the model transport error and representation error. We ignored the instrumental error, as did *Prinn et al.* [2001], since this is relatively small. Errors for the different sites and months were assumed to be uncorrelated. For the transport error, we used a formulation similar to that used by *Palmer et al.* [2003], assuming that the relative residual error, or the standard error of the differences between the model and observed daily means for a given month and site, reflects errors in model transport. For the representation error, which accounts for the mismatch between the point measurements and the concentrations in the larger model grid boxes, we used a formulation similar to that of *Chen* [2003], computing the standard deviation of the model monthly means for the grid box and the four surrounding grid boxes (at the same altitude). Since the grid boxes are narrower in the east-west direction toward the poles, we aggregated a number of adjacent boxes in calculating the representation errors for the sites Barrow and South Pole (3 adjacent boxes for Barrow, 9 to 24 adjacent boxes for South Pole). Transport errors across all sites were in the range of 0.05% to 3.5%, and representation errors were between 0.008% and 12%, with total observation errors between 0.06% and 13%, or 0.08 ppt and 19 ppt (1σ). The observation errors were generally much smaller for the ESRL South Pole site than the other sites (by about an order of magnitude or more), since it is far removed from pollution sources and exhibits little short-term variability. Because of the very unequal weighting that would result from the inclusion of the South Pole data, we omitted those data in the final analysis. (This is discussed further in section 3.2.)

[16] We tested also an alternative formulation for the observation error that generates values that are larger and more even across the sites, allowing us to retain the South Pole data in the inversion. This formulation, similar to that used by *Wang et al.* [2004], assumed that the transport error is simply a constant percentage, 2%, of the average concentration observed for a given month and site. The representation error was approximated as the standard error of the monthly mean calculated from daily mean concentrations. Results using this alternative formulation are discussed in section 3.2.

[17] We carried out an observing system simulation experiment, similar to that described by *Jones et al.* [2003], as an initial test to ascertain that the parameters can be constrained by the information contained in the observations, given the associated uncertainty estimates. In brief, the method involved specifying a set of "true" parameter values, and generating a set of a priori parameter estimates and many sets (e.g., 50) of synthetic observations using our Jacobian matrix and errors randomly picked from normal distributions scaled to the uncertainty estimates; the inverse calculation was then applied to these data. We found that the inversion was able to return results close to the "true" values on average, especially for the global OH parameter, verifying that sufficient information is contained in the observations.

3. Results

3.1. Simulation of Pollution Events

[18] A comparison of model and observed daily average MCF concentrations for a sampling of sites and years is shown in Figure 1 to illustrate model performance. (Model results here reflect optimized sources and sinks for MCF; we discuss the inversion results in depth below.) Figure 1 includes sites from both networks (Cape Grim, Cape

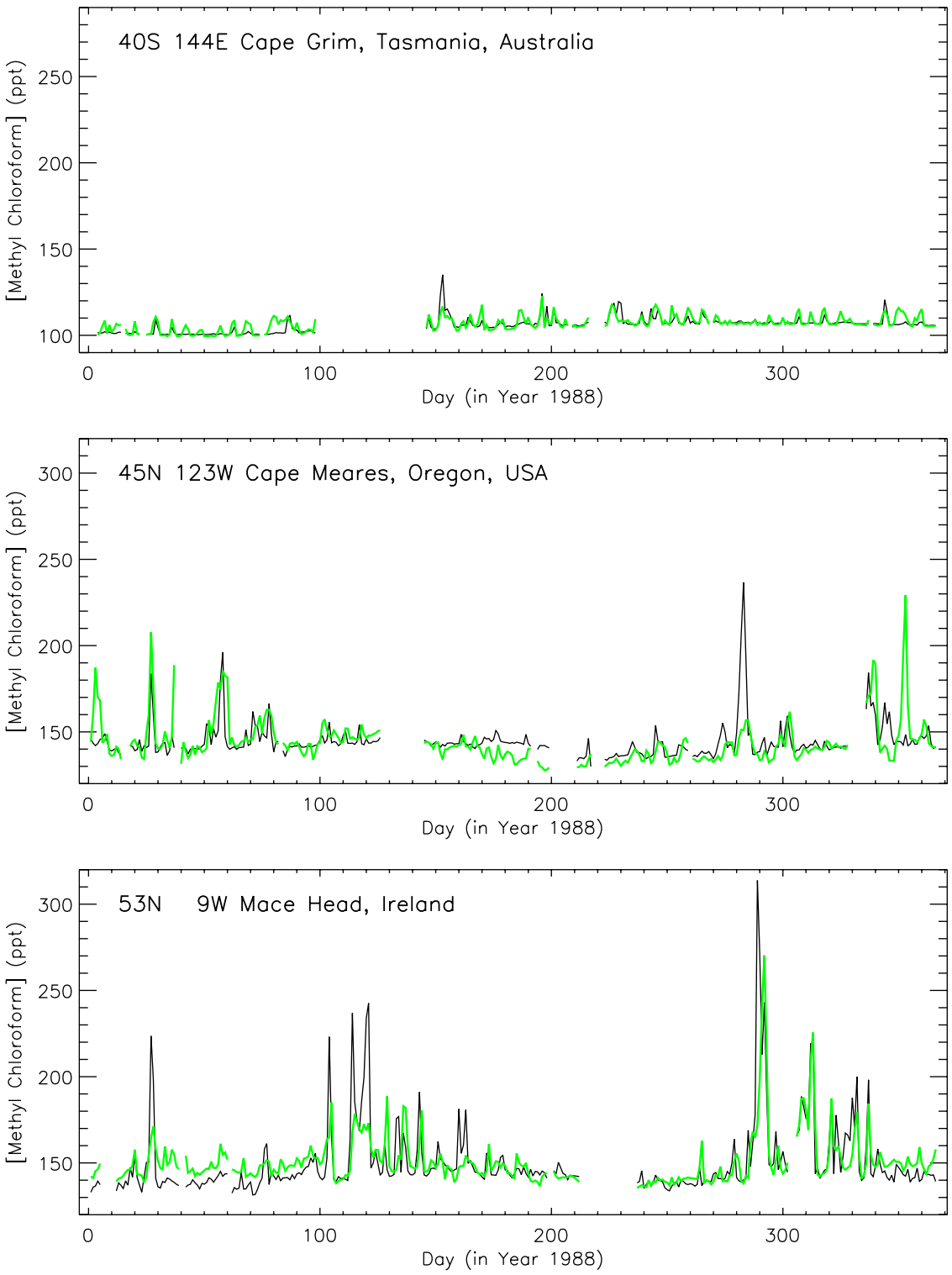

Figure 1. Comparison of model and observed daily average MCF concentrations for a sampling of sites and years. Thin black lines represent observations, and thick green lines represent the model. Gaps in the time series represent missing observations.

Meares, and Mace Head from GAGE and Niwot Ridge from ESRL), ranging from clean to occasionally polluted. In general, the model exhibits spikes in MCF concentration close to when they are found in the observations and also captures periods with relatively clean air. The model matches the timing and magnitude of many of the observed day-to-day fluctuations at all sites. We calculated simple statistics to assess the magnitude of biases in the model simulation of pollution spikes. For Mace Head, the most polluted site, the model underestimates "polluted" concen-

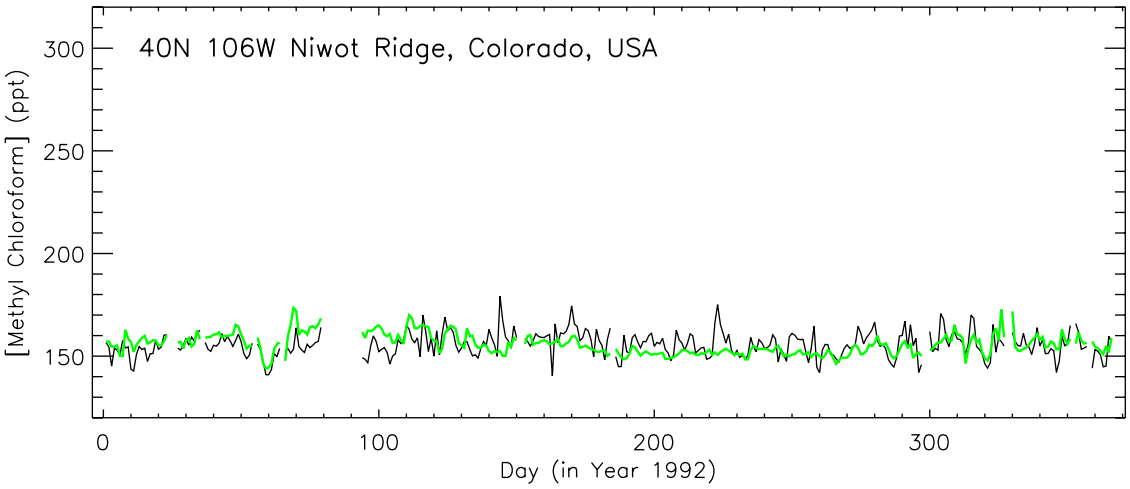

Figure 1. (continued)

trations (which we define in this calculation as model or observed daily values that are more than 1 standard deviation above the annual mean) on average by 14 ppt, or 7%, during 1988. For Cape Meares, another relatively polluted site, the model overestimates "polluted" concentrations on average by 7 ppt, or 4%, during 1988. These statistics suggest that the model does not consistently underestimate pollution spikes at all sites, as might be expected of a global model.

[19] The model does have specific shortcomings. For example, the model has smaller fluctuations at Niwot Ridge in the summer than observed. This station is located on a mountain ridge subject to shifts between clean downslope and more polluted upslope airflow, complexity that is difficult to capture in a model with $4^\circ \times 5^\circ$ resolution. But overall, the results give us confidence that the pollution events can be included usefully in the analysis, enabling a better estimate of regional sources than can be obtained using only background concentrations. In section 3.4.4, we discuss tests in which polluted data were filtered out.

3.2. Inversion Results

[20] Results for the first year of the inverse analysis, 1988, are shown in Figure 2. For the standard setup, the a posteriori global OH sink for MCF and global MCF source are both lower than the a priori estimates. The central value for the a priori OH sink lies outside of the 2σ uncertainty range of the a posteriori estimate, suggesting a significant decrease in OH relative to the prior estimate.

[21] The averaging kernels for the inversion, or model resolution functions, are displayed in Figure 3. Specifically, element A_{ij} of the averaging kernel matrix gives an indication of the sensitivity of the estimated magnitude of parameter i to the unknown true magnitude of parameter j; in the ideal case, **A** would be an identity matrix, without any correlation between different parameters [*Kasibhatla et al.*, 2002]. (We provide the formula for **A** in Appendix A.) The lines in Figure 3 represent individual rows of **A**; lines between points do not have any physical meaning. The averaging kernel for the OH parameter is sharply peaked with a value close to 1, indicating that global OH is well constrained and exhibits little correlation with source parameters. On the other hand, the sources in the NH tropics and the SH are not well constrained; however, these are relatively small, since there is little industrial activity in these regions. There is some correlation among the other NH sources. The result for total global emissions is more robust, as indicated by the averaging kernel for the aggregated global emissions: with two parameters, global emissions and global OH, the averaging kernels are both strongly peaked, with values of 0.74 for the source parameter and 0.97 for the sink parameter (not shown in Figure 3). The correlations between the parameters (off-diagonal elements of **A**) are relatively small: -0.02 and -0.22 for the source and sink rows, respectively. The a posteriori global source and sink strengths for the aggregated source inversion are very close to those for the standard inversion, as can be seen in Figure 2.

[22] We present in Figure 4 a comparison of model and observed MCF concentrations for the different sites. As expected, the inversion improves the agreement between model and observations on average. The improved agreement is reflected also in the normalized chi-square (cost function) values before and after the inversion, as shown in Table 2. The expected value for a satisfactory retrieval is 1; that is, the tightness of fit of the inversion results to the observations and to the a priori parameter estimates is comparable to the level of uncertainty assumed for the observations and the a priori estimates [*Marks and Rodgers*, 1993].

[23] The inversion results are presented in a more instructive format in Figure 5, which displays latitude profiles of annual mean MCF concentrations. It is apparent that the a priori interhemispheric gradient is too large, with concentrations too high in the NH and too low in the SH. To reduce the gradient, the inversion reduces emissions, lowering concentrations at the NH sites, and reduces OH, increasing concentrations at the SH sites (the SH is not influenced much by local emissions); the lowering of OH also maintains a global mass balance for MCF. In summary, the inversion results are driven largely by the need to correct for an excessive interhemispheric gradient in addition to the requirement for mass balance. We arrived at a similar conclusion in our analysis of the CH_4 budget [*Wang et*

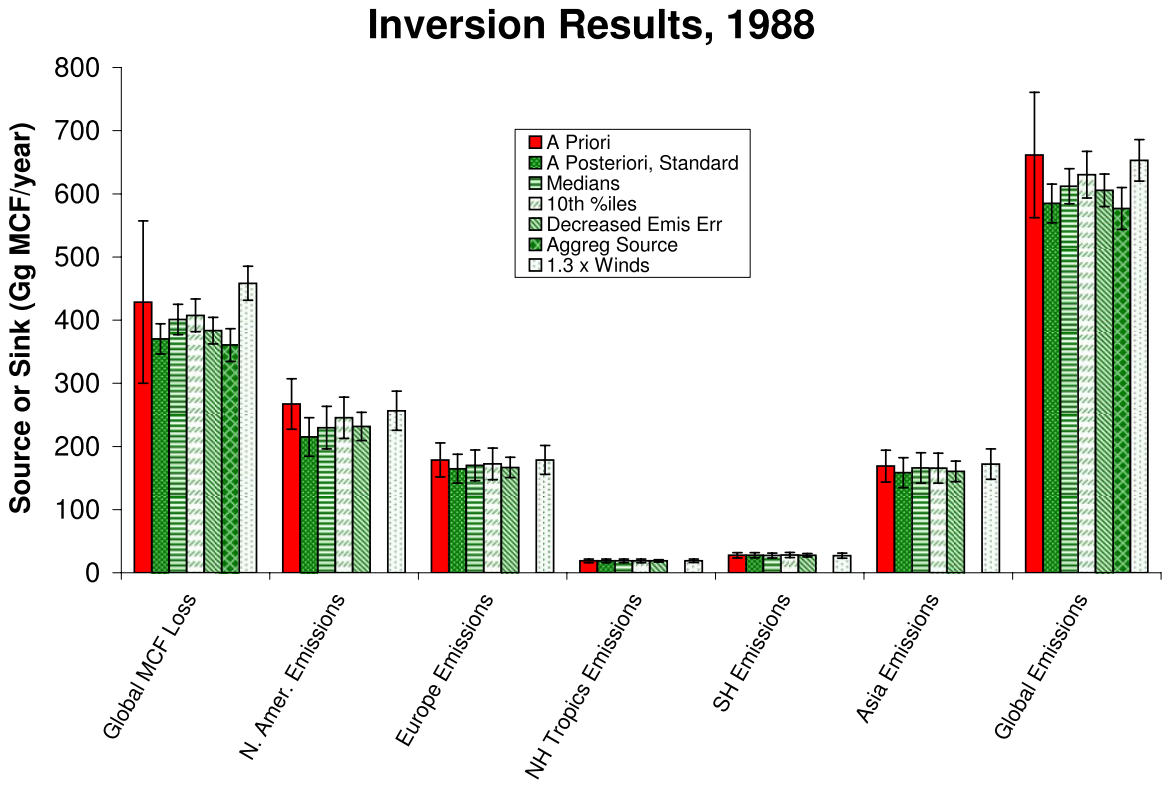

Figure 2. Inversion results, 1988 (GAGE). The results labeled "Medians" used monthly median data rather than monthly means, "10th %iles" used monthly 10th percentile data rather than means, "Decreased Emis Err" assumed a priori uncertainties for emissions of 5% instead of 7.5%, "Aggreg Source" combined all source parameters into a single parameter, and "1.3 x Winds" used a CTM run in which winds in the tropics were increased by a factor of 1.3. The error bars represent the 2σ uncertainty ranges.

al., 2004]: an excessive latitudinal gradient requires a decrease both in sources and global OH. Previous studies of CH_4 did not optimize concentrations of OH or severely restricted the degree to which OH could be adjusted.

[24] Results for the inversion using 1992 ESRL data are presented in Figures 4 and 5. As mentioned in section 2, the observation errors for the South Pole (SPO) site are much smaller than those for all other ESRL sites in our particular error formulation. As a consequence, the SPO data are weighted very heavily in the inversion, while not much use is made of the information from other sites. When the SPO data are included, the a posteriori agreement between model and observations is poor for most sites other than SPO; in contrast, the agreement between model and observations is good for most sites when SPO is excluded (Figure 4b). The chi-square values for the two inversions confirm that omitting data from SPO results in a better overall fit (Table 2).

[25] However, the a posteriori chi-square is still much greater than 1 when SPO is excluded (8.7); this result suggests that our standard error formulation generates observation errors that are too small (particularly for the ESRL sites) in addition to being uneven across sites. Nevertheless, we decided to retain our error formulation and exclude the SPO site in all of our standard inversions using ESRL data, rather than artificially tuning the errors to produce a desirable chi-square value, as has been done in some previous studies [e.g., *Bousquet et al.*, 2005]. We were encouraged that results from the standard inversion analysis are consistent with those for a number of other inversions with different setups. For example, similar results were obtained from an analysis using our alternative observation error formulation (Figure 6); recall from section 2 that these errors are larger and more similar in magnitude across the sites, including SPO. Figures 4c and 5c show comparisons of model and observed MCF concentrations for the inversion using alternative observation errors. Table 2 indicates that the a posteriori chi-square for this inversion, 1.4, is close to the expected value of 1. Figure 6 shows that results were also similar when we used the 1992 GAGE data, as well as when we used the combined GAGE-ESRL data set (excluding SPO), adjusted to compensate approximately for the differences in the standard scales.

[26] For the 1992 ESRL inversion, as for the 1988 GAGE inversion, the excessive a priori interhemispheric gradient (Figures 5b and 5c) leads to a reduction in the global source and in the magnitude of the OH sink. In essence, two pieces of information, the global MCF budget and the latitudinal gradient, uniquely determine the strengths of both the OH sink and the emissions.

3.3. Results for All Years and Comparison With Previous Studies

[27] A posteriori MCF emissions for all years of the analysis are shown in Figure 7. The results obtained using

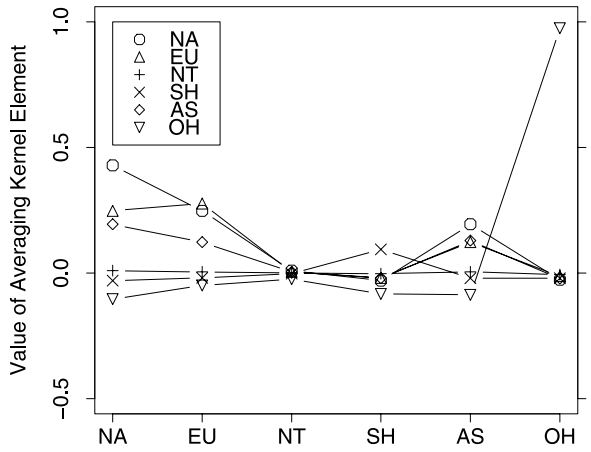

Figure 3. Averaging kernels (model resolution functions) for 1988 inversion. NA, North America emissions; EU, Europe emissions; NT, Northern Hemisphere tropics emissions; SH, Southern Hemisphere emissions; AS, Asia emissions; and OH, MCF loss due to OH.

the GAGE and ESRL data sets agree with each other for the years in which they overlap. Both sets of a posteriori emissions are consistently lower than the a priori values taken from *McCulloch and Midgley* [2001]. The discrepancy decreases after 1990, the year in which the London Amendment to the Montreal Protocol was adopted, after which global MCF emissions began to decline. Before 1990, the a posteriori emissions are on average 12% lower than the a priori values, while after 1990 the a posteriori emissions average 9% lower than a priori values. Interestingly, a similar result was obtained by *Simmonds et al.* [1996], albeit for one particular region, using a completely different approach: they analyzed polluted air masses moving over Mace Head, Ireland using a simple back-trajectory model, and derived an estimate for MCF emissions from Europe that is on average ∼9% lower than that of *Midgley and McCulloch* [1995] between 1987 and 1993. In comparison, our inversion results for Europe are on average 13% lower than Midgley and McCulloch for the period 1988–1993.

[28] *Bousquet et al.* [2005] also inferred a smaller global source than estimated by *McCulloch and Midgley* [2001] between 1988 and 1994 (in fact for most of the other years between 1980 and 1995 as well). However, the decrease is smaller than in our inversion, probably due in part to the tighter constraint they place on the emissions. They assumed the uncertainties quoted by *McCulloch and Midgley* [2001], which are generally 2–2.5%, except after the early 1990s, when emissions decreased and associated uncertainties increase in percentage terms. Before 1990, their a posteriori emissions are on average 2% lower than McCulloch and Midgley, while after 1990 the a posteriori emissions also average 2% lower than McCulloch and Midgley. In a test in which they placed a tighter constraint on monthly OH (uncertainty of 15% instead of 100%) while leaving the emissions uncertainties unchanged, the decrease in emissions relative to a priori is larger, with their a posteriori emissions being on average 4% lower than McCulloch and Midgley pre-1990 and 3% lower post-1990.

[29] Results for the lifetime of MCF with respect to tropospheric OH are shown in Figure 8 for all of the years of our analysis. (The lifetime is defined here as the atmospheric burden of MCF divided by loss due to tropospheric OH. The troposphere is taken to be the region beneath the climatological annual mean tropopause as diagnosed by the lapse rate in the GEOS-1 meteorological data.) Calculated lifetimes are generally longer than those reported by *Spivakovsky et al.* [2000] and *Prinn et al.* [2005]. Although Prinn et al. accounted for the possibility that a portion of the MCF manufactured was emitted with a longer lag time than

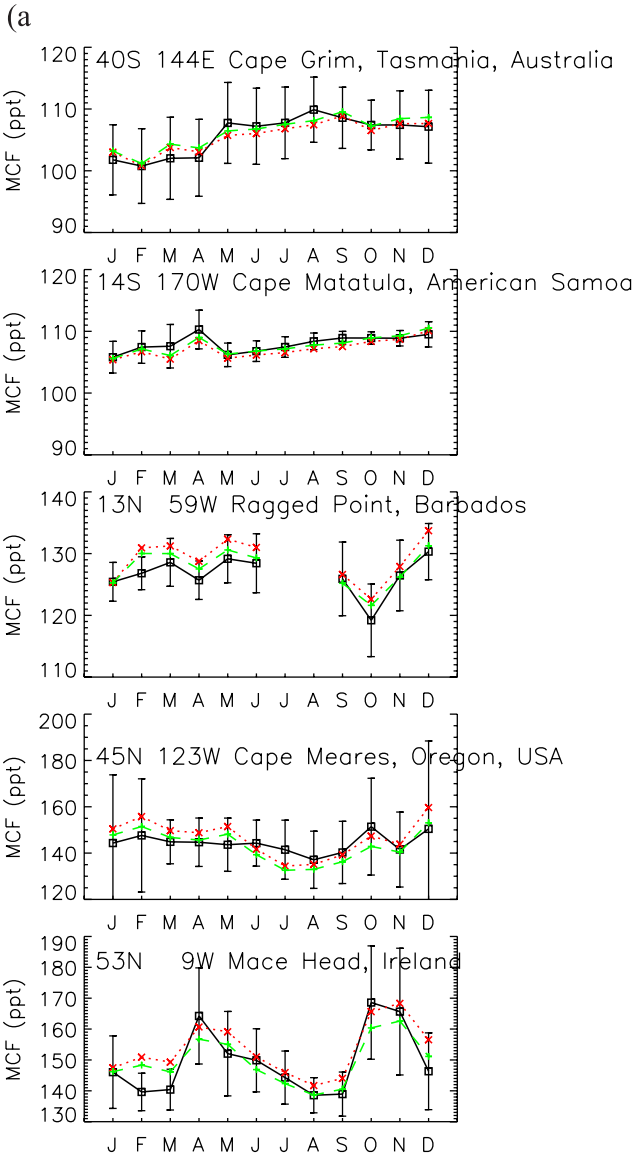

Figure 4. Comparison of model and observed MCF concentrations. (a) 1988 (GAGE). (b) 1992 (ESRL, standard observation errors, without South Pole site). (c) 1992 (ESRL, alternative observation errors, with South Pole site). Black squares/solid lines represent observations, red crosses/dotted lines represent model a priori, and green pluses/dashed lines represent model a posteriori. Error bars represent 2σ uncertainty ranges.

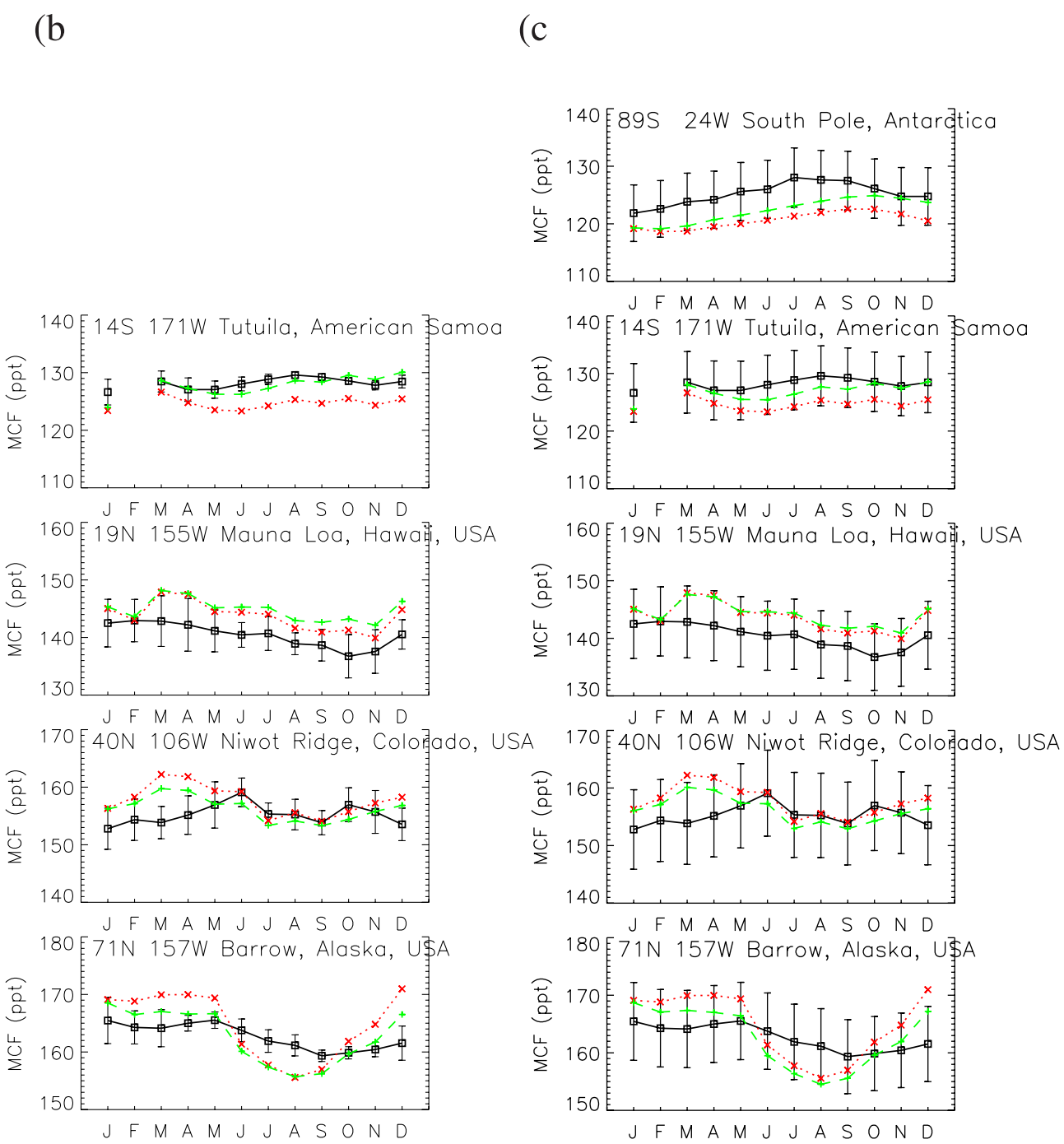

Figure 4. (continued)

assumed by *McCulloch and Midgley* [2001] (5% emitted after 10 years), the resulting adjustments to the emissions estimates of McCulloch and Midgley were quite small, ranging from −0.46 to −2.67 Gg/a between 1988 and 1991 and from +0.83 to +7.51 Gg/a between 1992 and 1994. (Note that these "reference" emissions are actually halfway between the "5% delayed" scenario and the estimates of McCulloch and Midgley.) Thus, the emissions assumed by Prinn *et al.* are nearly the same as those of McCulloch and Midgley. We discuss in detail the possibility of an underestimated lag time for emissions in section 4.1.

[30] Calculated lifetimes from both the present study and *Prinn et al.* [2005] exhibit sizable interannual fluctuations, suggesting that the two analyses interpret the interannual variations in the observations in a similar manner, with the differences attributable primarily to an overall offset in lifetimes resulting from the reduction in emissions implied by the present study. (The interannual variations in emissions are similar in the two analyses, except that our emissions exhibit a smaller relative decrease between 1993 and 1994, consistent with our relatively short MCF lifetime (high OH) in 1994.) Various factors contribute to

Table 2. Normalized Chi-Square (Cost Function) Values for Selected Inversions

Inversion	A Priori	A Posteriori
1988 GAGE	1.5	0.8
1989 GAGE	3.2	1.3
1989 GAGE, fixed (unoptimized) emissions	3.1	1.7
1992 ESRL, including SPO (standard observation error)	501.1	118.0
1992 ESRL, excluding SPO (standard observation error)	29.7	8.7
1992 ESRL, alternative observation error, including SPO	2.3	1.4
1992 GAGE (standard observation error)	3.8	1.4

interannual variability of OH abundance and tracer lifetimes, including column ozone abundance, emissions of CO, hydrocarbons, NO_x, and aerosols, and meteorology [*Dentener et al.*, 2003; *Wang et al.*, 2004; *Prinn et al.*, 2005]. The sequence of interannual variations in OH or lifetime obtained from the inversion studies deviates significantly from that obtained from bottom-up, photochemical calculations [e.g., *Dentener et al.*, 2003; *Wang et al.*, 2004]. The amplitude of the interannual fluctuations in our inversion results is also larger than that in bottom-up calculations and that derived from simple mass balance calculations based on observations of atmospheric CH_4 [*Lelieveld et al.*, 2006]. For example, our results using the GAGE data exhibit an average year-to-year variability of 20%, while the average variability of MCF lifetime with respect to the bottom-up OH fields used by *Wang et al.* [2004] is 2.5% and the average variability of OH estimated from CH_4 mass balance is on the order of 2%; the average variability for the results of *Prinn et al.* [2005] during 1988–1994 is 12%, also quite large. Possible explanations include errors inherent in the inversion approach [*Krol and Lelieveld*, 2003; *Bousquet et al.*, 2005] and errors in the characterization of factors contributing to OH variability in photochemical calculations. However, the focus of this paper is on differences in long-term average OH among studies rather than on interannual variability of OH, and we believe that the long-term average OH derived from our inverse analysis is a more robust quantity, since year to year variations in errors due to factors such as winds can be expected to cancel out to a certain extent. Support for this idea is provided by the analysis of *Krol and Lelieveld* [2003], who retrieved similar

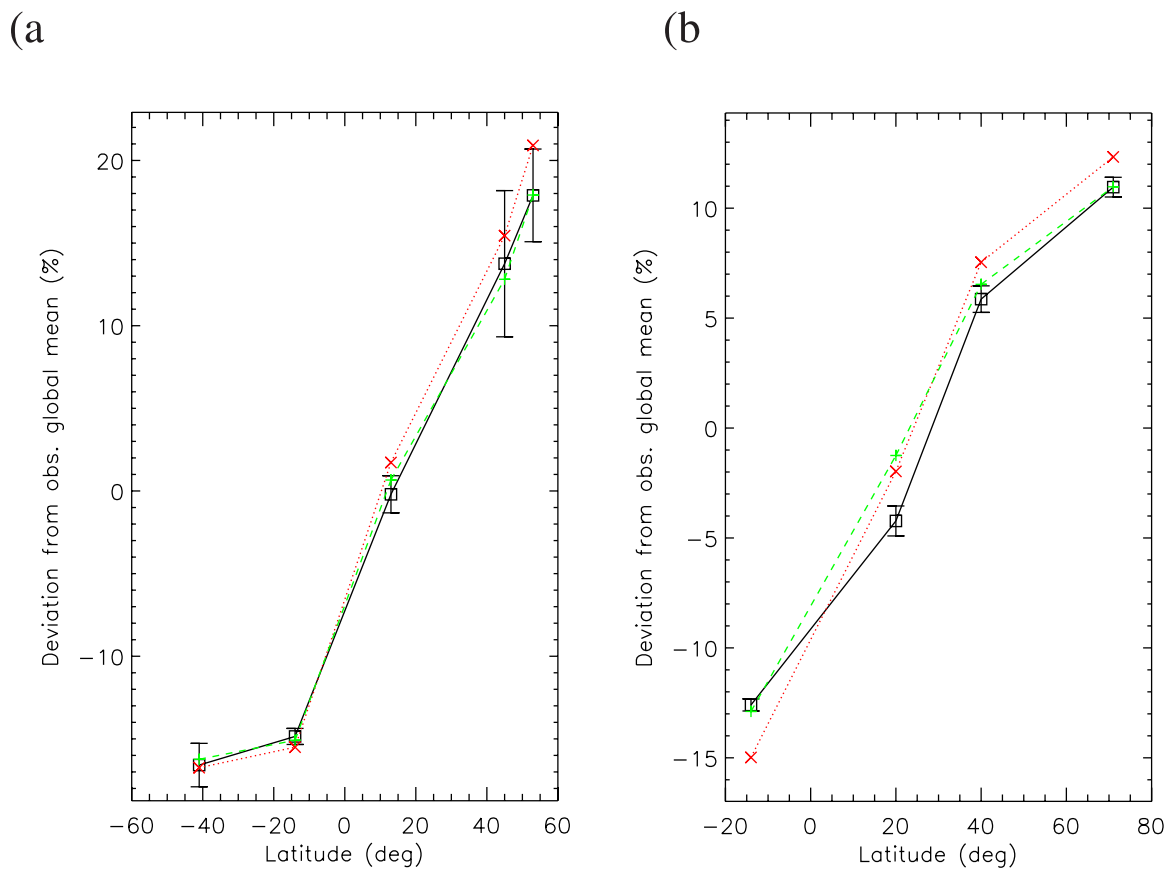

Figure 5. Latitudinal profiles of annual mean MCF concentrations. (a) 1988 (GAGE). (b) 1992 (ESRL, standard observation errors, without South Pole site). (c) 1992 (ESRL, alternative observation errors, with South Pole site). (d) For sensitivity test with wind speeds in tropics increased by a factor of 1.3, year 1988 (GAGE). Black squares/solid lines represent observations, red crosses/dotted lines represent model a priori, and green pluses/dashed lines represent model a posteriori. Error bars represent 2σ uncertainty ranges.

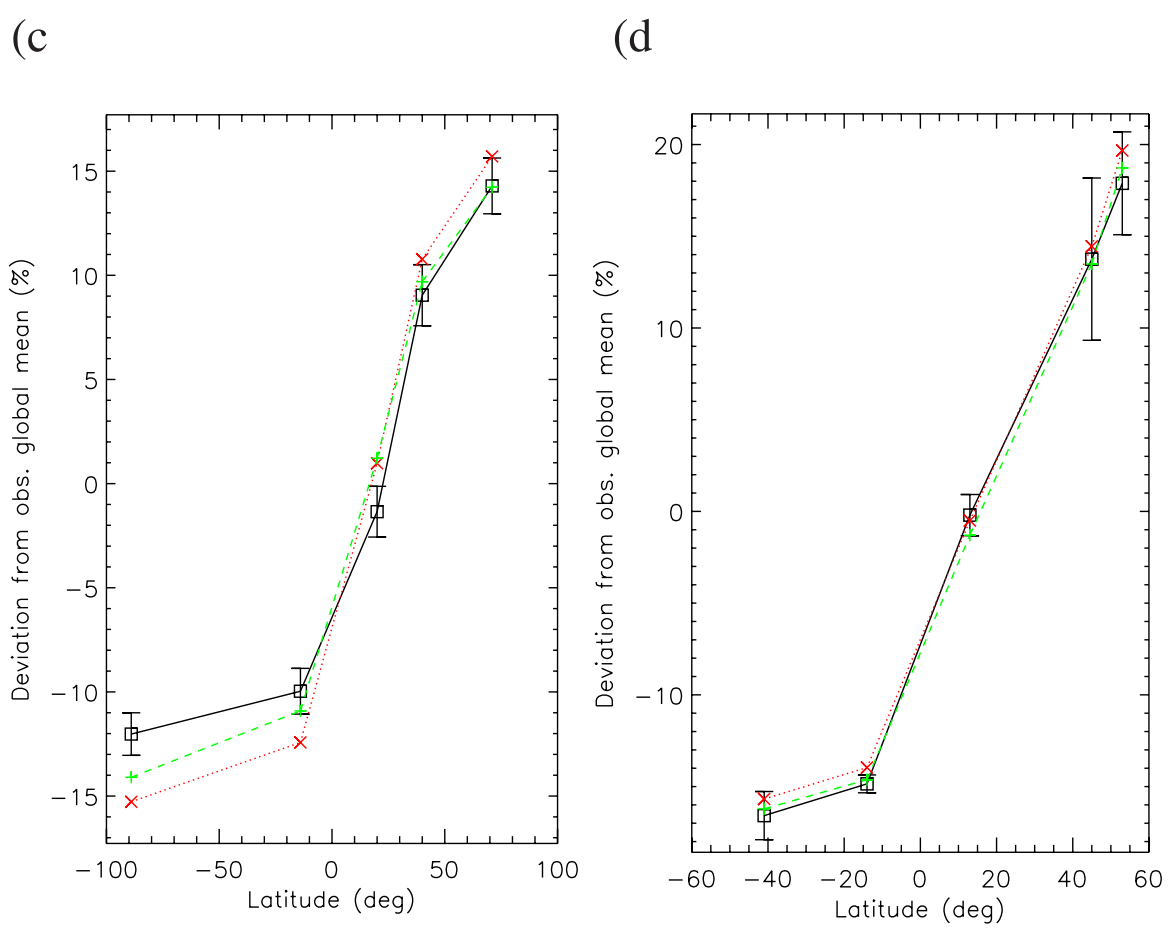

Figure 5. (continued)

long-term trends in global OH using either 1-, 3-, or 5-year optimization intervals or a second-order polynomial covering the entire 23-year period.

[31] Table 1 summarizes overall results for tropospheric mean OH and trace gas lifetimes, along with estimates reported in previous studies. We do not include values for lifetime for the study by *Bousquet et al.* [2005] in the table, since that paper reported only OH concentrations and not optimized lifetimes. However, on the basis of the a priori lifetime for CH_4 with respect to OH of 8 years that they reported, assuming that their definition for lifetime is the same as that in our Table 1, and using the ratio of MCF lifetime to CH_4 lifetime from our study, we estimate that their average a posteriori MCF lifetime (over the period 1980–2000) is 5.9 years, similar to other previous estimates.

[32] The value for mean OH derived here (weighted by air mass) is lower than some of the values obtained in the previous studies (but higher than others). Lifetimes for MCF (with respect to tropospheric OH) and CH_4 (with respect to all sinks) are 11–21% and 10–20% longer, respectively, than results reported in the previous studies. Note that a particular study may report a comparatively short lifetime but also a comparatively low value for mean OH, e.g., *Krol and Lelieveld* [2003] and possibly *Bousquet et al.* [2005]. A likely explanation is that discrepancies can arise between the mean OH concentrations reported by different studies due simply to differences in model domain and spatial resolution and in the weighting used (e.g., by air mass versus by rate of reaction with MCF) [*Lawrence et al.*, 2001]. The relationship between mean OH and MCF lifetime also depends on the vertical and spatial distributions of OH and temperature, which vary among models. Thus, we focus here on the comparison of lifetimes, which are also more directly inferred from MCF observations than are OH concentrations.

[33] Our standard inversion suggests that the lifetime of CH_4 could be 16% longer than the value recommended by the IPCC AR4 (Table 1). Similarly, an increase, by 6%, is implied by the analysis of *Prinn et al.* [2005]. Independent support for a lengthening of pollutant lifetimes is provided by *Montzka et al.* [2000], who estimated a lifetime for MCF based on the rate of decay of observed atmospheric concentrations during the late 1990s (when emissions were low and their uncertainty has a smaller effect on the lifetime estimate), and found it to be longer than previous estimates by 8% or more. We cannot compare our MCF lifetime directly with that estimated by Montzka et al., since the time periods are distinct. But for the sake of making a comparison, let us assume here that the lifetime did not change significantly between the two periods. Then combining the values for the lifetimes with respect to tropospheric OH, stratospheric loss, ocean uptake, and the soil sink from our analysis of 6.9 years, 45 years, 85 years, and 45 years, respectively (the soil sink is derived below in section 4.1.),

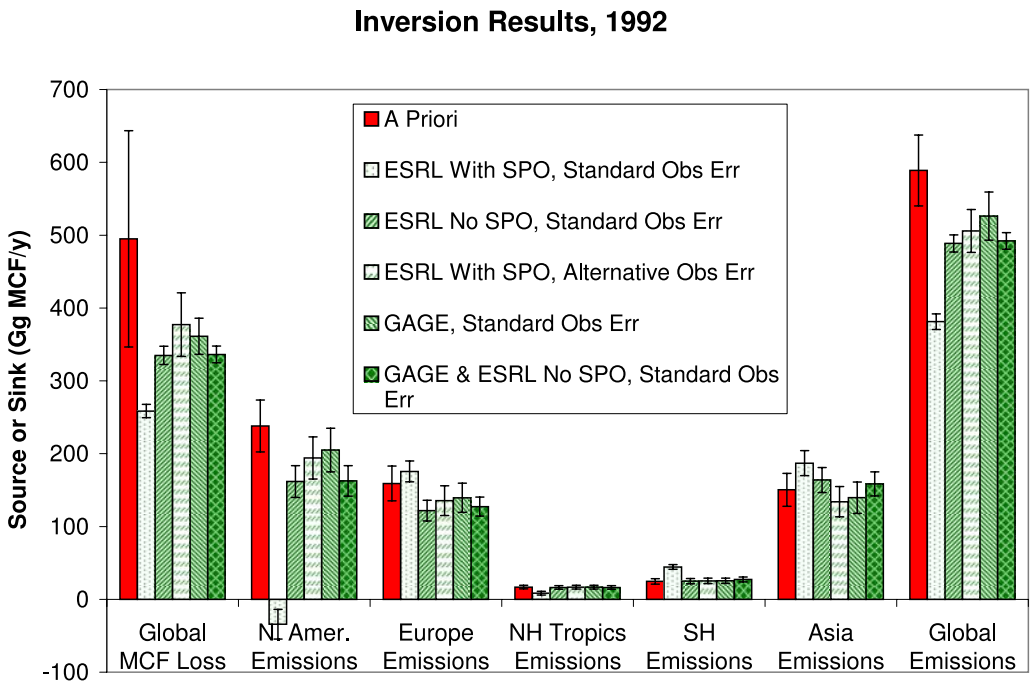

Figure 6. Inversion results for 1992 using various data sets and observation error formulations. For the results labeled "ESRL With SPO, Alternative Obs Err," errors assigned to the SPO observations were more comparable in magnitude to those for the other stations; for "GAGE & ESRL No SPO, Standard Obs Err," the GAGE and ESRL data were adjusted to compensate for the differences in the standard scales and used simultaneously. Error bars represent 2σ uncertainty ranges.

we obtain an overall MCF lifetime of 5.0 years. This lies within the upper limit to the MCF lifetime of 5.5 years calculated by Montzka et al., which assumes zero MCF emissions. This is also consistent with their best guess of 5.2 (+0.2, −0.3) years, which accounts for a small amount of emissions as estimated from industrial data. Thus, our estimated lifetime appears to be consistent with the constraint from the observed decay of atmospheric MCF, with the caveat that the time periods differ. Previous studies obtained overall lifetimes for MCF ranging from 4.6 to 5.1 years (for varying analysis periods) [*Spivakovsky et al.*, 2000; *Krol and Lelieveld*, 2003; *Prinn et al.*, 2005].

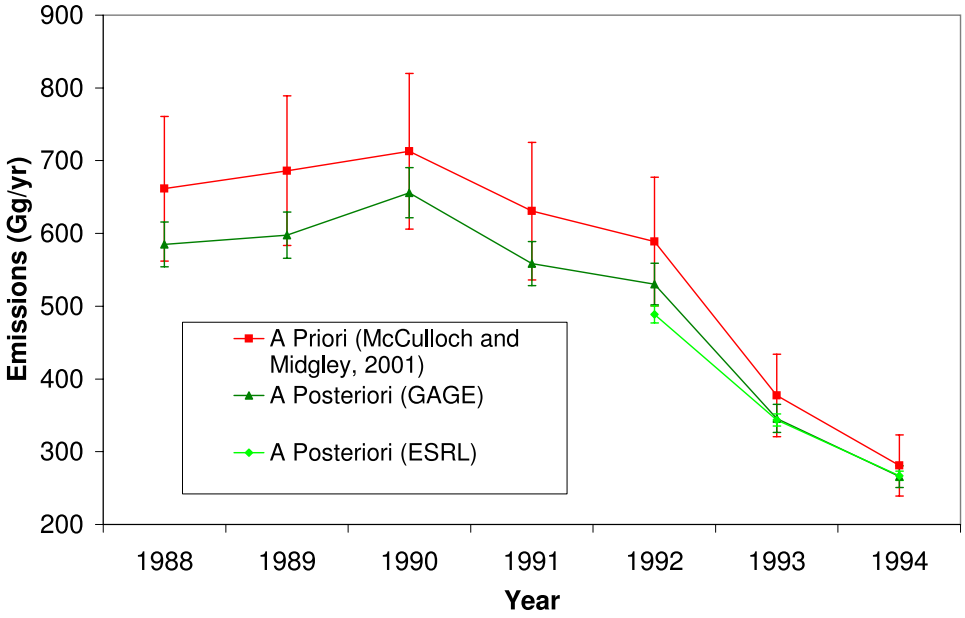

Figure 7. Comparison of a priori and a posteriori global MCF emissions, 1988–1994. Error bars represent 2σ uncertainty ranges. The London Amendment to the Montreal Protocol, which mandated a phase-out of MCF production, was adopted in 1990.

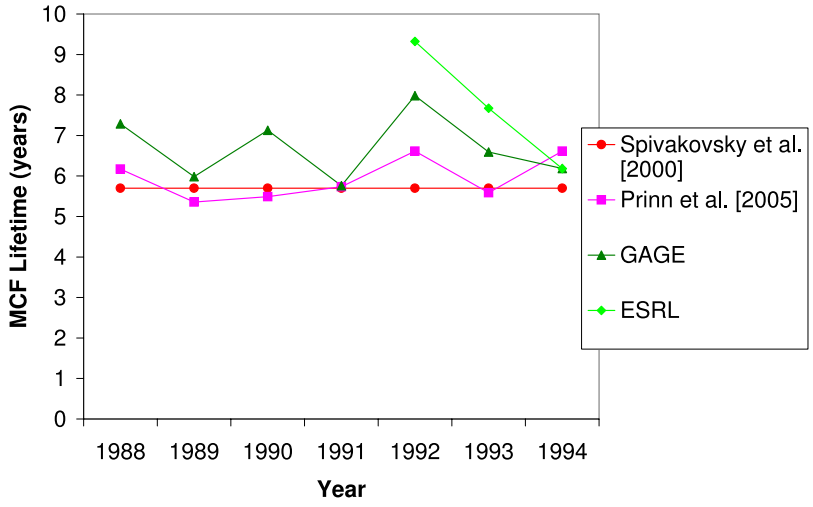

Figure 8. Global MCF lifetime with respect to OH, 1988–1994. We derived the annual lifetimes for *Prinn et al.* [2005] from the reported annual OH concentrations and overall lifetime for their analysis period, assuming that the lifetimes are inversely proportional to the OH concentrations.

3.4. Critical Uncertainties Affecting the Estimation of Global OH

[34] Our standard inversion produces estimates for MCF emissions and lifetime with respect to tropospheric OH that are substantially different from previous estimates, and the results are driven by an a priori overestimate of the interhemispheric gradient. Here, we explore why our results are different from previous studies and the sensitivity of our results to the model and to our assumptions.

3.4.1. Optimization of Emissions

[35] Allowing emissions to be optimized plays an important role, as we suggested in the introduction. To test the possibility that an adjustment of the interhemispheric distribution of OH, without an adjustment of emissions, could result in a similar fit of the model to the observations, we carried out an inversion in which the emissions were fixed (not optimized). As expected from mass balance, the a posteriori MCF lifetime with respect to tropospheric OH for 1989, 5.1 years, is shorter than that derived from the global OH inversion with optimized emissions, 6.0 years. However, we note that the fixed emissions inversion produces an inferior a posteriori fit to the observations, as can be inferred from the chi-square values in Table 2 for the 1989 inversions. (We show this comparison for 1989 rather than 1988 since the contrast is more noticeable.) Fixing emissions also necessitates a large adjustment of the OH distribution, resulting in an a posteriori NH/SH ratio for OH of 1.3, compared to the a priori of 0.9. The ratio of 1.3 is also large compared to the 0.9 for a hemispheric OH inversion with optimized emissions and is on the high end of the range found in the literature, including a range of 0.8–1.0 from other inversion studies [*Prinn et al.*, 2001; *Krol and Lelieveld*, 2003; *Bousquet et al.*, 2005], 1.0–1.3 from other photochemical model calculations [*Hauglustaine et al.*, 1998; *Spivakovsky et al.*, 2000; *Krol and Lelieveld*, 2003; *Bloss et al.*, 2005; *Jöckel et al.*, 2006], and a value of 0.88 from a photochemical model constrained to ground-based observations of OH concentrations [*Bloss et al.*, 2005].

[36] We do not discuss in detail results of inversions in which OH in the NH and SH were allowed to be independent, adjustable parameters, *and* emissions were optimized, since we found a significant degree of correlation between the OH and source parameters in the NH, as mentioned in section 2. However, it is interesting to note that in these inversions, OH generally decreased on a global average relative to the a priori value (with a greater decrease in the SH than in the NH for most years). This suggests that given the freedom to adjust emissions, the inversion tends to decrease them and global OH, despite the fact that a change in the interhemispheric distribution of OH alone can bring the model concentrations close to observations.

[37] We tested also the effect of a smaller a priori uncertainty for emissions (5% instead of 7.5% (1σ)). As expected, the a posteriori parameter estimates did not deviate as far from the a priori as in the standard inversion (Figure 2), although they are still ~10% less for 1988. *Bousquet et al.* [2005], while allowing emissions to be adjusted, placed an even tighter constraint on them in all their inversions, as we described above. Their a priori uncertainties were generally 2–2.5% except after the early 1990s. This could be one factor contributing to the smaller decrease in emissions relative to a priori in their study than in ours.

3.4.2. Rate of Interhemispheric Mixing

[38] Given that our inversion results are driven by the need to match the observed interhemispheric gradient of MCF, it is reasonable to expect that the results will be sensitive to the rate of interhemispheric mixing in the CTM. Despite the reasonable simulations of ^{85}Kr and SF_6 by GEOS-Chem, there are uncertainties in the observations and noticeable discrepancies between model and observed profiles. For example, in the simulations of SF_6 latitudinal profiles shown in Figure 9, the model gradient in the tropical Pacific is not as sharp as that in the observations, while the model overestimates the overall gradient in the Atlantic.

[39] To assess the influence of the rate of interhemispheric mixing on the inversion results, we carried out a test in

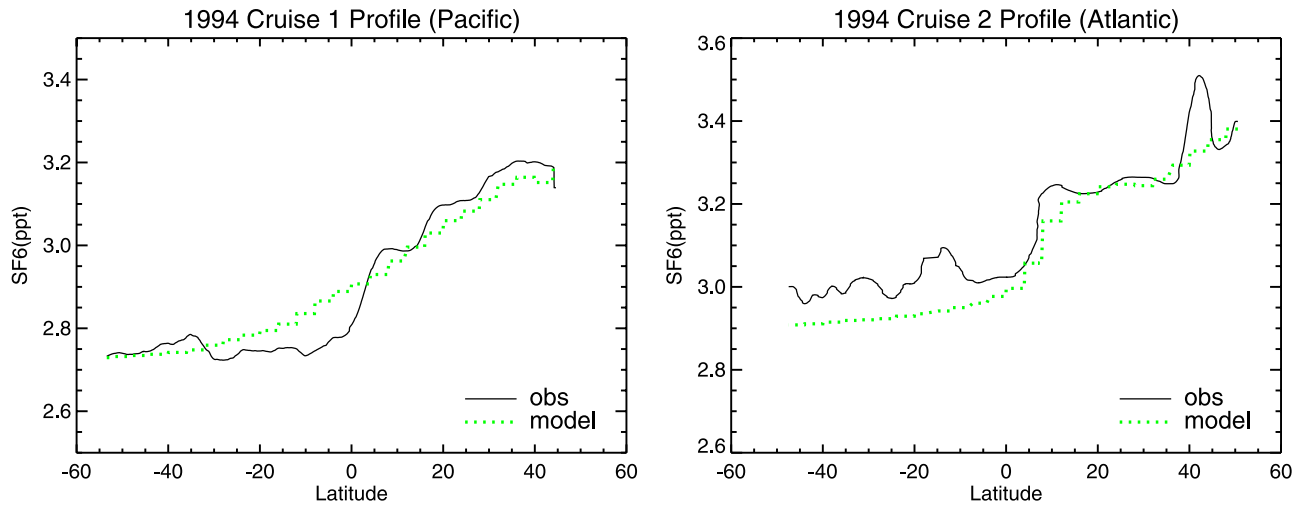

Figure 9. Comparison of model latitudinal profile of SF_6 with observations from two cruises in 1994. Smoothed observations provided by *Geller et al.* [1997] are used here. Model results are averaged over the longitudinal extent and time period of the cruises.

which we arbitrarily increased wind speeds in the tropics (between 20°S and 20°N) uniformly by 30%. This causes the interhemispheric exchange time for MCF to decrease substantially for 1988, from 0.86 to 0.69 years, or 20%. We found that the increased mixing reduced the a priori interhemispheric gradient of MCF so that it was no longer larger than the observed gradient (see Figure 5d). Not surprisingly, the a posteriori source and sink strengths are not very different from the a priori; in fact, the optimized sink is larger than the a priori (Figure 2). However, it is likely that the agreement between model and observed profiles of ^{85}Kr and SF_6 would be worsened by this large increase in mixing.

[40] The CTM used by *Bousquet et al.* [2005] had an interhemispheric exchange time of ~0.87 years for ^{85}Kr [*Hauglustaine et al.*, 2004], 21% shorter than the 1.1 years reported by *Jacob et al.* [1987] and 13% shorter than our 1.0 years. (Hauglustaine et al. actually reported an exchange time of 0.82 years, but their definition for exchange time did not account for atmospheric sinks for the tracer; we used *Jacob et al.* [1987, equation 7] and assumed a radioactive decay time of 15.52 years to convert the exchange time to one that can be compared directly with those from the other studies.) Hauglustaine et al. also reported that their exchange time for fossil fuel CO_2, 1.13 years, lay at the low end of the range exhibited in an intercomparison of 12 models, 1.06–2.14 years. Bousquet et al. indeed noted that the mixing in their model was relatively fast and that their optimized model underestimates the gradient of MCF between Ragged Point, Barbados and Cape Grim, Tasmania. We hypothesize that smoothing of the latitudinal gradient due to the relatively fast mixing in the model of Bousquet et al. contributes to their relatively small decrease in emissions relative to a priori and their possible lack of an increase in MCF lifetime.

3.4.3. Interhemispheric Distribution of OH

[41] We tested also the response to an alternative a priori OH field, on the basis of a calculation with the kinetic solver (rather than the parameterization) in the GEOS-Chem CTM (v. 4.33) [*Fiore et al.*, 2003]. (Although the OH field is derived from a run for year 2001, we were interested here in any contrasting distribution rather than one calculated specifically for our analysis period.) The alternative field had an average NH to SH ratio for OH of 1.08, as compared to a value of 0.94 for the standard field. The global source and OH sink are 3% and 2% higher, respectively, than those from the standard inversion for year 1994. While this appears to be a relatively small effect, we found in section 3.4.1 that a NH to SH ratio for OH of 1.3 and fixed emissions could produce reasonable agreement between model and observed latitudinal gradients. A ratio of 1.3 has been seen in at least one photochemical model [*Bousquet et al.*, 2005], though it is larger than many other estimates in the literature, as discussed in section 3.4.1.

3.4.4. Simulation of Pollution Events

[42] As mentioned in section 2., previous MCF inversion studies used data from which pollution events had been filtered out (with the exception of one sensitivity test in the work by *Bousquet et al.* [2005]), while we kept the polluted data. The GEOS-Chem model simulates pollution events, as demonstrated in Figure 1, but inevitably there are discrepancies. These discrepancies include overall negative or positive biases in the pollution events at different sites as well as problems specific to a particular site and time of year, as was detailed in section 3.1. To assess the influence of biases in the CTM's simulation of pollution events as well as investigating the effect of keeping polluted data on the inversion results, we carried out inversions using monthly median and monthly 10th percentile concentrations instead of monthly means for both model output and observations; this procedure, in effect, filters out a good portion of the polluted data. We calculated that for Mace Head, the polluted means are on average 9 ppt higher than the unpolluted means (provided on the GAGE website) during 1988–1989, the medians are 4 ppt higher than the unpolluted means, and the 10th percentiles are 2 ppt lower than the unpolluted means. (The average value for the unpolluted means during 1988–1989 is 143 ppt.) For Cape Meares, the polluted means are on average 3.5 ppt higher than the unpolluted, the medians are 1 ppt higher, and the

10th percentiles are 2 ppt lower. (The average for the unpolluted means during 1988 is 141 ppt; there is only partial data for 1989.)

[43] Using the 1988 medians, the resulting a posteriori global source and sink due to OH are only ~1% higher than in the standard inversion (Figure 2). Carrying out the extreme test using the very clean 10th percentiles, we obtained a small 5% decrease in the global OH sink relative to the a priori and a 5% decrease in global emissions (Figure 2).

[44] In another test, we omitted the Niwot Ridge data, since the complex pollution events at that site were difficult for the model to capture. We found that for year 1992, the global source and sink due to OH are only 0.1% and 0.4% higher, respectively, than in the standard inversion.

[45] It appears that the inversion results are sensitive to the simulation of pollution events, although the sensitivity is not as large as that for the other factors discussed above.

4. Discussion

4.1. Hypothesis for the Discrepancy Between a Priori and a Posteriori Emissions Estimates

[46] We emphasize that the decrease in global emissions obtained in our standard inversion is based on a particular set of assumptions and on the transport characteristics of the GEOS-Chem CTM. Thus, it may be premature to lay out a hypothesis as to the cause of the discrepancy. But we do so in the following to show that a lowering of emissions estimates could be consistent with other findings in the literature.

[47] The discrepancy between a posteriori and a priori emissions estimates appears, at first glance, to be large and difficult to explain, given that the latter are based on industry sales data, which are presumably accurate, and that MCF is a highly volatile liquid thought to be emitted completely to the atmosphere within 3 years of purchase [*McCulloch and Midgley*, 2001]. We hypothesize, however, that the discrepancy results from a combination of two factors: (1) an underestimate by *McCulloch and Midgley* [2001] of the delay between MCF sales and emissions and (2) the presence of a soil sink and/or other sinks for MCF (such as destruction in incinerators, landfills) that were not accounted for in previous inverse studies. We expound on this hypothesis in the remainder of this section.

[48] If all of MCF was emitted completely to the atmosphere within 3 years of purchase, emissions should closely track sales and should have declined close to zero in much of the world, including North America and Europe, by the late 1990s [*McCulloch and Midgley*, 2001]. However, a number of groups have observed unexpectedly high atmospheric concentrations of MCF over North America and Europe as recently as the late 1990s and early 2000s [*Millet and Goldstein*, 2004; *Barnes et al.*, 2003; *Krol et al.*, 2003; *Li et al.*, 2005] and over Japan in 2002 [*Yokouchi et al.*, 2005]. These investigators suggested the possibility of an underestimate of the time lag between MCF sales and emissions, and offered a number of plausible explanations, including suggestions of an underestimate of stockpiling of the chemical shortly before the phase-out of production, intensified efforts at recycling, and slow release from aerosol containers and landfills. E. Hodson et al. (personal communication, 2004) detected significant concentrations of MCF in landfill gas from a site in the eastern U.S. in 2003. In light of these observations, *Prinn et al.* [2005] considered the possibility that 5% of the MCF manufactured could have taken as long as 10 years to enter the atmosphere. A delay in emissions could account for the convergence with time between the a priori and a posteriori emissions in our analysis.

[49] A delay in emissions alone would not appear to account for the entire discrepancy between a priori and a posteriori emissions, however, since the a posteriori results are still less than the a priori values by the end of the analysis period. Improbably large additional emissions would be required after 1994 (at least 400 Gg) to account for all the MCF sold in the past. Loss of MCF in the presence of various types of clay particles has been detected and quantified under a variety of conditions in the laboratory by *Kutsuna et al.* [2000, 2003]. Given that the reaction rate increases with increasing temperature and decreases with increasing relative humidity, the investigators suggested that significant loss of MCF would most likely occur in hot and arid or semiarid regions with large amounts of exposed clay particles; they speculate that this soil sink for MCF could significantly affect its overall atmospheric lifetime. The soil sink would appear to be associated loosely with MCF emissions geographically, since the majority of hot, arid land areas occur in the subtropics and midlatitudes of the NH, the latitudes where much of the emission occurs. Thus, our inverse calculation would interpret the combination of emissions and a soil sink as a decrease in (net) emissions relative to the a priori. Since there have been no field experiments that we are aware of with the express purpose of detecting a soil sink for MCF, this idea remains speculative.

[50] We carried out a set of simple calculations to estimate the magnitude of a hypothetical soil sink. We assumed first that the difference between the a posteriori and a priori emissions would be attributed entirely to removal by soils. Resulting values for the lifetime of MCF with respect to loss in soils are plotted in Figure 10, the curve labeled "McCulloch and Midgley Central Emissions." Notice that the curve suggests a steep upward temporal trend in the lifetime associated with the soil sink. Since a large temporal trend in lifetime seems unreasonable, we took into account then the possible delay in emissions discussed above by considering a shift in some of the emissions from earlier to later; specifically, we calculated soil sink lifetimes corresponding to *McCulloch and Midgley*'s [2001] lower and upper bound emissions estimates (-2σ and $+2\sigma$). These curves are included also in Figure 10. It is apparent that if the lower bound emissions are assumed at the beginning of the period, the central emissions in the middle, and the upper bound emissions at the end, the inferred soil sink lifetime would be approximately constant over the period, corresponding to a value of about 45 years. This value lies close to center of the range of lifetimes estimated by *Kutsuna et al.* [2003]. Shifts in emissions implied by this analysis would correspond to a decrease of about 30 Gg (−4%) for both 1988 and 1989, an increase of about 60 Gg (+15%) for 1993, and an increase of about 40 Gg (+16%) for 1994. We do not quantify here the

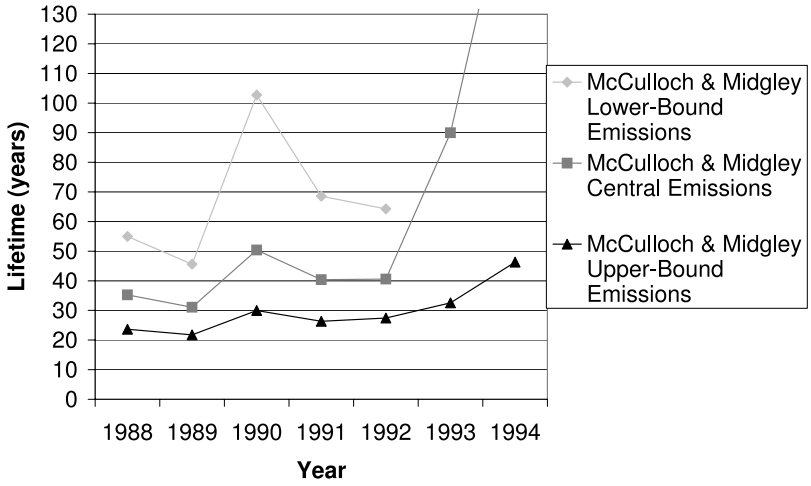

Figure 10. Estimated lifetimes of MCF with respect to a possible soil sink. See text for an explanation of the methodology. (Values for 1993–1994 for the case of lower bound emissions are not shown since they are negative.)

emissions changes for years before and after our period of analysis.

[51] In summary, the lower (net) emissions inferred for MCF relative to a priori values (especially pre-1990) are consistent with an underestimate of the delay between MCF sales and emissions in combination with removal by a possible soil sink neglected previously.

4.2. Global OH Calculated by Photochemical Models

[52] One explanation for a possible overestimate of global OH in older, bottom-up photochemical calculations [e.g., *Spivakovsky et al.*, 2000] is the use of reaction rate coefficients and chemical mechanisms that have since been revised. Of particular interest is the upward revision of the rate for the $O(^1D) + N_2$ reaction, estimated to decrease OH production by 15% in the middle to upper troposphere [*Ravishankara et al.*, 2002]. A newer version of the GEOS-Chem model (run with fully interactive chemistry rather than prescribed OH fields) that includes the revised rate coefficient as well as other updates indicates a reduction in global mean OH by 9% with an 11% longer MCF lifetime, compared to an older version of the model with the same meteorological fields (Table 1, GEOS-Chem version 5.02 compared to version 4.26). Note that the precise value of the MCF lifetime in the GEOS-Chem model depends on the set of meteorological fields used. The model has been driven in various studies by meteorological fields from several versions of the assimilation system: GEOS-1 for 1988–1995, GEOS-Strat for 1996–2000, GEOS-3 for 1998 and 2000–2002, and GEOS-4 since 2001 (http://www-as.harvard.edu/chemistry/trop/geos/geos_sim.html). Changes in meteorological fields cause changes in mean OH in part via significantly different cloud distributions. For example, mean OH decreased by 4% using the same model version (5.05.03) for GEOS-3 fields for 2001 compared to GEOS-Strat fields for 1996 (H. Liu, personal communication, 2004). A recent comparison of simulations for 2001 showed an increase of 9% in mean OH using GEOS-4 fields compared to GEOS-3 fields, as shown in Table 1 [*Wu et al.*, 2007].

4.3. Implications of Findings for Trace Gases Budgets and Climatic Impacts

[53] Future work narrowing critical uncertainties could help confirm or disprove the results of our standard inversion. If our finding is confirmed, it would provide a revised benchmark against which to evaluate the output of global photochemical models, as well as possibly resolving imbalances in the budgets of a number of trace gases. Analyses of tracers other than MCF and CH_4 also suggest a need to lower OH. For example, *Spivakovsky et al.* [2000] report that large corrections in hemispheric OH would be needed to reconcile model and observed concentrations of dichloromethane (CH_2Cl_2) for years 1994–1996, assuming industry estimates for emissions: the interhemispheric gradient computed for CH_2Cl_2 is otherwise too large. The required corrections remain large when the rate of interhemispheric mixing in the CTM is increased to its upper limit consistent with observations of CFCs and ^{85}Kr. Alternatively, we propose that reduction in global OH and CH_2Cl_2 emissions would possibly improve the agreement between model and observations. Industrial and consumer uses for CH_2Cl_2 are similar to those for MCF [*McCulloch and Midgley*, 1996]. It seems plausible that net emissions have been overestimated for both gases.

[54] With a lower global abundance of OH, a given input of a species removed by OH results in a larger increase in concentration. Or conversely, a given reduction in emissions will result in a larger decrease in concentration than would have been the case with the shorter lifetime. Despite the adjustment in the lifetime of CH_4 and total emissions, our inverse estimate for the anthropogenic portion of current emissions (in Tg/a) remained close to that determined in bottom-up analyses [*Wang et al.*, 2004]. Thus, a given fractional decrease in anthropogenic CH_4 emissions would have a greater climate impact than assumed previously. But if emissions were to increase significantly [e.g., *Wang et al.*, 2004], the climate impact would also be greater.

[55] Global warming potential (GWP) is a measure, used in IPCC assessments, of the relative radiative effect of the emissions of a particular greenhouse gas. An increase in the

atmospheric lifetimes for CH_4, HFCs, and HCFCs would translate into an increase in their GWPs. In the case of CH_4, the 16% increase in lifetime, relative to the value reported in the IPCC Fourth Assessment Report, implied by our results translates approximately into a 16% increase in the GWP, from 25 to 29 (relative to CO_2, for a 100-year time horizon). This assumes no change in the ratio of the perturbation lifetime (which accounts for chemical feedbacks resulting from an addition of CH_4 to the atmosphere and is what is actually used to calculate GWP) to the atmospheric lifetime (atmospheric burden divided by rate of loss) [*Denman et al.*, 2007].

5. Conclusions

[56] MCF emissions from our standard inversion are about 10% lower than published inventories on average between 1988 and 1994, and the decrease in the global sink due to OH suggested by the inversion implies an average lifetime for MCF (with respect to tropospheric OH) of about 6.9 years, 11–21% longer than the 5.7–6.2 years reported in previous optimization studies. Our results contradict the high level of understanding on global lifetimes of pollutants that might be implied by the ±4% range of the estimates for MCF lifetime cited above.

[57] Our inversion results are driven by the need to match the observed latitudinal gradient of MCF, while balancing the MCF budget. The relatively loose a priori constraint we placed on MCF emissions, the rate of interhemispheric mixing in our particular CTM, the interhemispheric distribution of OH assumed, and the CTM's simulation of pollution events are critical, uncertain factors that contributed to the low values for global emissions and global OH in our standard inversion. The sensitivity tests we carried out show that plausible alternative assumptions and model characteristics can lead to results similar to those in previous studies. The alternative assumptions are generally extreme or lie on outer bounds of ranges in the literature though, as in the case of a rate of interhemispheric mixing similar to that in the CTM of *Hauglustaine et al.* [2004] or a NH to SH ratio for OH of 1.3 combined with fixed emissions. We note that we have conducted simulations of ^{85}Kr and SF_6 to assess the interhemispheric transport in our CTM, and it appears satisfactory. We believe it is important that future inverse studies take care to present results of simulations of ^{85}Kr, SF_6, and possibly other tracers and to report values for MCF lifetime and mean OH that can be compared unambiguously with values from previous studies.

[58] We recommend that future studies on OH abundance using alternative tracers such as HFC-134a, HCFC-141b, HCFC-142b, and HCFC-22 [*Huang and Prinn*, 2002; *O'Doherty et al.*, 2004] give special attention to allowing emissions and OH to be estimated simultaneously in inverse calculations rather than fixing one or the other. At present, there are significant uncertainties in the magnitudes and trends of the emissions for the alternative tracers listed above, which could be narrowed through the recommended inverse calculation.

[59] In future work, a useful analysis would be to conduct the inversions at higher spatial and temporal (e.g., week by week) resolution to clarify our understanding of the impact of inaccuracies in simulating pollution episodes on these findings. Field measurements and global process-based modeling of the soil sink for MCF would be helpful. With a fuller understanding of the distribution of the soil sink, an inverse analysis could reassess the global strength of the soil sink and could test our hypothesis for the discrepancy between a priori and a posteriori emission estimates.

[60] Our methods could be applied to a longer series of MCF observations to help confirm or disprove the results from our standard inversion as well as to assess the effect of lower OH concentrations and adjusted MCF emissions on long-term trends in OH. Particularly interesting would be an extension of our analysis forward into the late 1990s, as there has been lively debate about the effect of the assumed trend in MCF emissions on the deduced OH trend for the 1990s [e.g., *Prinn et al.*, 2001, 2005; *Krol and Lelieveld*, 2003; *Wang et al.*, 2004; *Millet and Goldstein*, 2004; *Bousquet et al.*, 2005].

Appendix A

A1. SF_6 Simulation

[61] In addition to the simulation of ^{85}Kr described by *Wang et al.* [2004], we carried out a simulation of SF_6 to evaluate the rate of interhemispheric mixing in the GEOS-Chem CTM. The distribution of SF_6 emissions was adopted from the EDGAR-95 data set [*Olivier and Berdowski*, 2001]. We scaled the global emissions for each year to match the observed annual growth of SF_6 in the atmosphere, a reasonable procedure given the uncertainty in the bottom-up emission estimates [see *Peters et al.*, 2004]. We determined the growth rate using observations for the following ESRL stations: South Pole, Cape Grim, Samoa, Mauna Loa, Niwot Ridge, Barrow, and Alert [*Geller et al.*, 1997]. The estimated emissions are 6750, 5163, and 6022 tons for years 1995–1997, respectively. We neglected loss of SF_6, an excellent approximation given the long lifetime of SF_6, 3200 years [*Ramaswamy et al.*, 2001].

[62] The model was initialized with hemispheric mean SF_6 mixing ratios derived from long-term observations at two sites [*Maiss and Levin*, 1994]. The model was spun up then from 1989 to 1991 to build up a self-consistent atmospheric distribution of SF_6. As expected, there were differences between model concentrations and observations for 1991 since the initial conditions and the magnitude and growth of the emissions during the spin-up years were not prescribed accurately. Model results at the end of 1991, after corrections for a globally uniform offset based on the observations available for this year [*Maiss and Levin*, 1994], were used to drive the simulation from 1992 to 1997. Our assessment of the interhemispheric mixing in the model relied on comparisons with observations for 1994–1997.

[63] The model results are compared in Figure 9 with observations from two cruises in 1994 [*Geller et al.*, 1997], one in the Pacific and one in the Atlantic. The model results displayed were averaged over the geographic extent and time period of the cruises [*Geller et al.*, 1997]. The size of the model interhemispheric gradient is comparable to that of the observations over both oceans, although the model gradient is not as sharp as observed in the Pacific and is slightly larger than observed in the Atlantic. Thus, there is some error in the simulation of interhemispheric mixing.

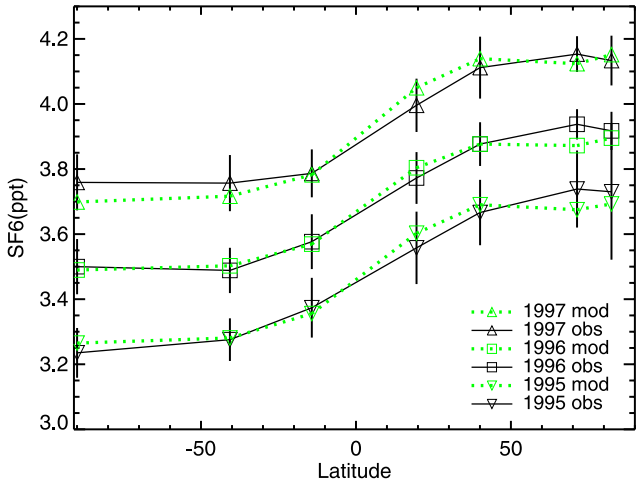

Figure A1. Comparison of model latitudinal profile of annual mean SF_6 concentrations with flask observations from ESRL sites, 1995–1997.

[64] Model results are compared in Figure A1 with annual mean ESRL flask measurements, available from 1995 onward for the seven sites listed above [*Geller et al.*, 1997]. We found good agreement between model and observations for all 3 years of the comparison, lending some confidence to the accuracy of interhemispheric exchange in the model.

[65] The agreement between the model and observed interhemispheric gradients of ^{85}Kr in the Atlantic lends further, albeit geographically and temporally limited, support to the accuracy of interhemispheric mixing in the model.

A2. Formula for Averaging Kernel Matrix

[66] The averaging kernel matrix, **A**, is given by

$$\mathbf{A} = \mathbf{GK}, \tag{A1}$$

where **G** is the gain matrix, and **K** is the Jacobian matrix.

[67] The gain matrix is given by

$$\mathbf{G} = \left(\mathbf{K}^T\mathbf{S}_\varepsilon^{-1}\mathbf{K} + \mathbf{S}_\mathbf{a}^{-1}\right)^{-1}\mathbf{K}^\mathrm{T}\mathbf{S}_\varepsilon^{-1}, \tag{A2}$$

where $\mathbf{S}\varepsilon$ is the observation error covariance matrix, and $\mathbf{S_a}$ is the a priori error covariance matrix.

[68] **Acknowledgments.** We thank Clarissa Spivakovsky, Dylan Jones, Jim Elkins, Maarten Krol, Philippe Bousquet, and Michael Prather for helpful discussions and suggestions. Yuhan Chen shared ideas on the inverse method. Jack Yatteau provided generous assistance with the computing system. We thank Ron Prinn for the GAGE MCF data and Jim Elkins, Jim Butler (SF_6), and Thayne Thompson (MCF) for the ESRL data. J.A.L. and I.A.M. were supported by the NASA ACMAP program.

References

Barnes, D. H., et al. (2003), Urban/industrial pollution for the New York City-Washington, D.C., corridor, 1996–1998: 2. A study of the efficacy of the Montreal Protocol and other regulatory measures, *J. Geophys. Res.*, *108*(D6), 4186, doi:10.1029/2001JD001117.

Bey, I., et al. (2001), Global modeling of tropospheric chemistry with assimilated meteorology: Model description and evaluation, *J. Geophys. Res.*, *106*, 23,073–23,096, doi:10.1029/2001JD000807.

Bloss, W. J., M. J. Evans, J. D. Lee, R. Sommariva, D. E. Heard, and M. J. Pilling (2005), The oxidative capacity of the troposphere: Coupling of field measurements of OH and a global chemistry transport model, *Faraday Discuss.*, *130*, 425–436, doi:10.1039/b419090d.

Bousquet, P., D. A. Hauglustaine, P. Peylin, C. Carouge, and P. Ciais (2005), Two decades of OH variability as inferred by an inversion of atmospheric transport and chemistry of methyl chloroform, *Atmos. Chem. Phys.*, *5*, 2635–2656.

Butler, J. H., J. W. Elkins, T. M. Thompson, B. D. Hall, T. H. Swanson, and V. Koropalov (1991), Oceanic consumption of CH_3CCl_3-Implications for tropospheric OH, *J. Geophys. Res.*, *96*, 22,347–22,355, doi:10.1029/91JD02126.

Chen, Y.-H. (2003), Estimation of methane and carbon dioxide surface fluxes using a 3-D global atmospheric chemical transport model, *Rep. 73*, MIT Cent. for Global Change Sci., Cambridge, Mass.

Denman, K. L., et al. (2007), Couplings between changes in the climate system and biogeochemistry, in *Climate Change 2007: The Physical Science Basis-Contribution of Working Group I to the Fourth Assessment Report of the Intergovernmental Panel on Climate Change*, edited by S. Solomon et al., pp. 499–587, Cambridge Univ. Press, New York.

Dentener, F., M. van Weele, M. Krol, S. Houweling, and P. van Velthoven (2003), Trends and inter-annual variability of methane emissions derived from 1979–1993 global CTM simulations, *Atmos. Chem. Phys.*, *3*, 73–88.

Duncan, B., D. Portman, I. Bey, and C. Spivakovsky (2000), Parameterization of OH for efficient computation in chemical tracer models, *J. Geophys. Res.*, *105*, 12,259–12,262, doi:10.1029/1999JD901141.

Fiore, A., D. J. Jacob, H. Liu, R. M. Yantosca, T. D. Fairlie, and Q. Li (2003), Variability in surface ozone background over the United States: Implications for air quality policy, *J. Geophys. Res.*, *108*(D24), 4787, doi:10.1029/2003JD003855.

Geller, L. S., J. W. Elkins, J. M. Lobert, A. D. Clarke, D. F. Hurst, J. H. Butler, and R. C. Myers (1997), Tropospheric SF6: Observed latitudinal distribution and trends, derived emissions and interhemispheric exchange time, *Geophys. Res. Lett.*, *24*(6), 675–678, doi:10.1029/97GL00523.

Hauglustaine, D. A., G. P. Brasseur, S. Walters, P. J. Rasch, J. F. Muller, L. K. Emmons, and C. A. Carroll (1998), MOZART, a global chemical transport model for ozone and related chemical tracers: 2. Model results and evaluation, *J. Geophys. Res.*, *103*(D21), 28,291–28,335.

Hauglustaine, D. A., F. Hourdin, L. Jourdain, M. A. Filiberti, S. Walters, J. F. Lamarque, and E. A. Holland (2004), Interactive chemistry in the Laboratoire de Meteorologie Dynamique general circulation model: Description and background tropospheric chemistry evaluation, *J. Geophys. Res.*, *109*, D04314, doi:10.1029/2003JD003957.

Huang, J., and R. G. Prinn (2002), Critical evaluation of emissions of potential new gases for OH estimation, *J. Geophys. Res.*, *107*(D24), 4784, doi:10.1029/2002JD002394.

Intergovernmental Panel on Climate Change (2001), in *Climate Change 2001: The Scientific Basis-Contribution of Working Group I to the Third Assessment Report of the Intergovernmental Panel on Climate Change*, edited by J. T. Houghton et al., Cambridge Univ. Press, New York.

Intergovernmental Panel on Climate Change (2007), *Climate Change 2007: The Physical Science Basis-Contribution of Working Group I to the Fourth Assessment Report of the Intergovernmental Panel on Climate Change*, edited by S. Solomon et al., Cambridge Univ. Press, New York.

Jacob, D. J., M. J. Prather, S. C. Wofsy, and M. B. McElroy (1987), Atmospheric distribution of ^{85}Kr simulated with a general circulation model, *J. Geophys. Res.*, *92*, 6614–6626, doi:10.1029/JD092iD06p06614.

Jöckel, P., et al. (2006), The atmospheric chemistry general circulation model ECHAM5/MESSy1: Consistent simulation of ozone from the surface to the mesosphere, *Atmos. Chem. Phys.*, *6*, 5067–5104.

Jones, D. B. A., K. W. Bowman, P. I. Palmer, J. R. Worden, D. J. Jacob, R. N. Hoffman, I. Bey, and R. M. Yantosca (2003), Potential of observations from the Tropospheric Emission Spectrometer to constrain continental sources of carbon monoxide, *J. Geophys. Res.*, *108*(D24), 4789, doi:10.1029/2003JD003702.

Karlsdóttir, S., and I. S. A. Isaksen (2000), Changing methane lifetime: Possible cause for reduced growth, *Geophys. Res. Lett.*, *27*, 93–96, doi:10.1029/1999GL010860.

Kasibhatla, P., A. Arellano, J. A. Logan, P. I. Palmer, and P. Novelli (2002), Topdown estimate of a large source of atmospheric carbon monoxide associated with fuel combustion in Asia, *Geophys. Res. Lett.*, *29*(19), 1900, doi:10.1029/2002GL015581.

Krol, M., and J. Lelieveld (2003), Can the variability in tropospheric OH be deduced from measurements of 1,1,1,-trichloroethane (methyl chloroform)?, *J. Geophys. Res.*, *108*(D3), 4125, doi:10.1029/2002JD002423.

Krol, M. C., J. Lelieveld, D. E. Oram, G. A. Sturrock, S. A. Penkett, C. A. M. Brenninkmeijer, V. Gros, J. Williams, and H. A. Scheeren (2003), Continuing emissions of methyl chloroform from Europe, *Nature*, *421*(6919), 131–135, doi:10.1038/nature01311.

Kutsuna, S., K. Takeuchi, and T. Ibusuki (2000), Laboratory study on heterogeneous degradation of methyl chloroform (CH3CCl3) on aluminosilica clay minerals as its potential tropospheric sink, *J. Geophys. Res.*, *105*, 6611–6620, doi:10.1029/1999JD901072.

Kutsuna, S., L. Chen, K. Ohno, N. Negishi, K. Takeuchi, T. Ibusuki, K. Tokuhashi, and A. Sekiya (2003), Laboratory study on heterogeneous decomposition of methyl chloroform on various standard aluminosilica clay minerals as a potential tropospheric sink, *Atmos. Chem. Phys.*, *3*, 1063–1082.

Lawrence, M. G., P. Joeckel, and R. von Kuhlmann (2001), What does the global mean OH concentration tell us?, *Atmos. Chem. Phys.*, *1*, 37–49.

Lelieveld, J., et al. (2006), New directions: Watching over tropospheric hydroxyl (OH), *Atmos. Environ.*, *40*, 5741–5743, doi:10.1016/j.atmosenv.2006.04.008.

Li, J., D. M. Cunnold, H.-J. Wang, R. F. Weiss, B. R. Miller, C. Harth, P. Salameh, and J. M. Harris (2005), Halocarbon emissions estimated from Advanced Global Atmospheric Gases Experiment measured pollution events at Trinidad Head, California, *J. Geophys. Res.*, *110*, D14308, doi:10.1029/2004JD005739.

Maiss, M., and I. Levin (1994), Global increase of SF_6 observed in the atmosphere, *Geophys. Res. Lett.*, *21*(7), 569–572, doi:10.1029/94GL00179.

Marks, C. J., and C. D. Rodgers (1993), A retrieval method for atmospheric composition from limb emission measurements, *J. Geophys. Res.*, *98*, 14,939–14,953, doi:10.1029/93JD01195.

Martin, R. V., D. J. Jacob, R. M. Yantosca, M. Chin, and P. Ginoux (2003), Global and regional decreases in tropospheric oxidants from photochemical effects of aerosols, *J. Geophys. Res.*, *108*(D3), 4097, doi:10.1029/2002JD002622.

McCulloch, A., and P. M. Midgley (1996), The production and global distribution of emissions of trichloroethene, tetrachloroethene and dichloromethane over the period 1988–1992, *Atmos. Environ.*, *30*, 601–608, doi:10.1016/1352-2310(09)50032-5.

McCulloch, A., and P. M. Midgley (2001), The history of methyl chloroform emissions: 1951–2000, *Atmos. Environ.*, *35*, 5311–5319, doi:10.1016/S1352-2310(01)00306-5.

Midgley, P. M., and A. McCulloch (1995), The production and global distribution of emissions to the atmosphere of 1,1,1-trichloroethane (methyl chloroform), *Atmos. Environ.*, *29*, 1601–1608, doi:10.1016/1352-2310(95)00078-D.

Millet, D. B., and A. H. Goldstein (2004), Evidence of continuing methylchloroform emissions from the United States, *Geophys. Res. Lett.*, *31*, L17101, doi:10.1029/2004GL020166.

Montzka, S. A., J. H. Butler, R. C. Myers, T. M. Thompson, T. H. Swanson, A. D. Clarke, L. T. Lock, and J. W. Elkins (1996), Decline in the tropospheric abundance of halogen from halocarbons: Implications for stratospheric ozone depletion, *Science*, *272*, 1318–1322, doi:10.1126/science.272.5266.1318.

Montzka, S. A., C. M. Spivakovsky, J. H. Butler, J. W. Elkins, L. T. Lock, and D. J. Mondeel (2000), New observational constraints for atmospheric hydroxyl on global and hemispheric scales, *Science*, *288*, 500–503, doi:10.1126/science.288.5465.500.

O'Doherty, S., et al. (2004), Rapid growth of hydrofluorocarbon 134a and hydrochlorofluorocarbons 141b, 142b, and 22 from Advanced Global Atmospheric Gases Experiment (AGAGE) observations at Cape Grim, Tasmania, and Mace Head, Ireland, *J. Geophys. Res.*, *109*, D06310, doi:10.1029/2003JD004277.

Olivier, J. G. J., and J. J. M. Berdowski (2001), Global emissions sources and sinks, in *The Climate System*, edited by J. Berdowski, R. Guicherit, and B. J. Heij, pp. 33–78, A. A. Balkema, Brookfield, Vt.

Palmer, P. I., D. J. Jacob, D. B. A. Jones, C. L. Heald, R. M. Yantosca, J. A. Logan, G. W. Sachse, and D. G. Streets (2003), Inverting for emissions of carbon monoxide from Asia using aircraft observations over the western Pacific, *J. Geophys. Res.*, *108*(D21), 8828, doi:10.1029/2003JD003397.

Peters, W., M. C. Krol, E. J. Dlugokencky, F. J. Dentener, P. Bergamaschi, G. Dutton, J. B. Miller, L. Bruhwiler, and P. P. Tans (2004), Toward regional-scale modeling using the two-way nested global model TM5: Characterization of transport using SF_6, *J. Geophys. Res.*, *109*, D19314, doi:10.1029/2004JD005020.

Prather, M., M. McElroy, S. Wofsy, G. Russell, and D. Rind (1987), Chemistry of the global troposphere: Fluorocarbons as tracers of air motion, *J. Geophys. Res.*, *92*, 6579–6613, doi:10.1029/JD092iD06p06579.

Prinn, R. G., et al. (2001), Evidence for substantial variations of atmospheric hydroxyl radical in the past two decades, *Science*, *292*, 1882–1888, doi:10.1126/science.1058673.

Prinn, R. G., et al. (2005), Evidence for variability of atmospheric hydroxyl radicals over the past quarter century, *Geophys. Res. Lett.*, *32*, L07809, doi:10.1029/2004GL022228.

Ramaswamy, V., O. Boucher, J. Haigh, D. Hauglustaine, J. Haywood, G. Myhre, T. Nakajima, G. Y. Shi, and S. Solomon (2001), Radiative forcing of climate change, in *Climate Change 2001: The Scientific Basis-Contribution of Working Group I to the Third Assessment Report of the Intergovernmental Panel on Climate Change*, edited by J. T. Houghton et al., pp. 349–416, Cambridge Univ. Press, New York.

Ravishankara, A. R., E. J. Dunlea, M. A. Blitz, T. J. Dillon, D. E. Heard, M. J. Pilling, R. S. Strekowski, J. M. Nicovich, and P. H. Wine (2002), Redetermination of the rate coefficient for the reaction of O (1D) with N2, *Geophys. Res. Lett.*, *29*(15), 1745, doi:10.1029/2002GL014850.

Reimann, S., et al. (2005), Low European methyl chloroform emissions inferred from long-term atmospheric measurements, *Nature*, *433*, 506–508, doi:10.1038/nature03220.

Schneider, H. R., D. B. Jones, G.-Y. Shi, and M. B. McElroy (2000), Analysis of residual mean transport in the stratosphere: I. Model description and comparison with satellite data, *J. Geophys. Res.*, *105*, 19,991–20,011, doi:10.1029/2000JD900213.

Simmonds, P. G., R. G. Derwent, A. McCulloch, S. O'Doherty, and A. Gaudry (1996), Long-term trends in concentrations of halocarbons and radiatively active trace gases in Atlantic and European air masses monitored at Mace Head, Ireland from 1987–1994, *Atmos. Environ.*, *30*, 4041–4063, doi:10.1016/1352-2310(96)00055-6.

Spivakovsky, C. M., et al. (2000), Three dimensional climatological distribution of tropospheric OH: Update and evaluation, *J. Geophys. Res.*, *105*, 8931–8980, doi:10.1029/1999JD901006.

Wang, J. S., J. A. Logan, M. B. McElroy, B. N. Duncan, I. A. Megretskaia, and R. M. Yantosca (2004), A 3-D model analysis of the slowdown and interannual variability in the methane growth rate from 1988 to 1997, *Global Biogeochem. Cycles*, *18*, GB3011, doi:10.1029/2003GB002180.

Wennberg, P. O., S. Peacock, J. T. Randerson, and R. Bleck (2004), Recent changes in the air-sea gas exchange of methyl chloroform, *Geophys. Res. Lett.*, *31*, L16112, doi:10.1029/2004GL020476.

World Meteorological Organization (2003), Scientific assessment of ozone depletion: 2002, *Global Ozone Res. Monit. Proj., Rep. 47*, Geneva, Switzerland.

Wu, S., L. J. Mickley, D. J. Jacob, J. A. Logan, R. M. Yantosca, and D. Rind (2007), Why are there large differences between models in global budgets of tropospheric ozone?, *J. Geophys. Res.*, *112*, D05302, doi:10.1029/2006JD007801.

Yokouchi, Y., T. Inagaki, K. Yazawa, T. Tamaru, T. Enomoto, and K. Izumi (2005), Estimates of ratios of anthropogenic halocarbon emissions from Japan based on aircraft monitoring over Sagami Bay, Japan, *J. Geophys. Res.*, *110*, D06301, doi:10.1029/2004JD005320.

W. L. Chameides, Nicholas School of the Environment and Earth Sciences, Duke University, Durham, NC 27708, USA.

J. A. Logan, M. B. McElroy, I. A. Megretskaia, and Y. Wang, Department of Earth and Planetary Sciences, Harvard University, Cambridge, MA 02138, USA.

P. I. Palmer, School of GeoSciences, University of Edinburgh, Edinburgh EH9 3JW, UK.

J. S. Wang, Environmental Defense Fund, New York, NY 10010, USA. (jwang@environmentaldefense.org)